

# Chemical abundance analysis of the open clusters Berkeley 32, NGC 752, Hyades, and Praesepe<sup>★</sup>

R. Carrera<sup>1,2,3,4</sup> and E. Pancino<sup>3</sup>

<sup>1</sup> Instituto de Astrofísica de Canarias, La Laguna, Tenerife, Spain  
e-mail: rcarrera@iac.es

<sup>2</sup> Departamento de Astrofísica, Universidad de La Laguna, Tenerife, Spain

<sup>3</sup> INAF-Osservatorio Astronomico di Bologna, Bologna, Italy

<sup>4</sup> Centro de Investigaciones de Astronomía, Mérida, Venezuela

Received September 15, 2110; accepted March 16, 2220

## ABSTRACT

**Context.** Open clusters are ideal test particles for studying the chemical evolution of the Galactic disc. However, the number and accuracy of existing high-resolution abundance determinations, not only of [Fe/H], but also of other key elements, remains largely insufficient.

**Aims.** We attempt to increase the number of Galactic open clusters that have high quality abundance determinations, and to gather all the literature determinations published so far.

**Methods.** Using high-resolution ( $R \sim 30000$ ), high-quality ( $S/N \geq 60$  per pixel), we obtained spectra for twelve stars in four open clusters with the fibre spectrograph FOCES, at the 2.2 Calar Alto Telescope in Spain. We employ a classical equivalent-width analysis to obtain accurate abundances of sixteen elements: Al, Ba, Ca, Co, Cr, Fe, La, Mg, Na, Nd, Ni, Sc, Si, Ti, V, and Y. We derived oxygen abundances derived by means of spectral synthesis of the 6300 Å forbidden line.

**Results.** We provide the first determination of abundance ratios other than Fe for NGC 752 giants, and ratios in agreement with the literature for the Hyades, Praesepe, and Be 32. We use a compilation of literature data to study Galactic trends of [Fe/H] and  $[\alpha/\text{Fe}]$  with Galactocentric radius, age, and height above the Galactic plane. We find no significant trends, but some indication for a flattening of [Fe/H] at large  $R_{gc}$ , and for younger ages in the inner disc. We also detect a possible decrease in [Fe/H] with  $|z|$  in the outer disc, and a weak increase in  $[\alpha/\text{Fe}]$  with  $R_{gc}$ .

**Key words.** Stars: abundances – Galaxy: disc – Galaxy: open clusters and associations: individual: NGC 752; Hyades; Berkeley 32; Praesepe (M 44)

## 1. Introduction

Open clusters (hereafter OC) are ideal *test particles* for studying the evolution of metallicity with time, inferring the so-called *age-metallicity relation*, and with Galactocentric radius, the *metallicity gradient*, measuring in the Galactic disc. Their properties can be determined with smaller uncertainties than for field stars, since they are coeval group of stars at the same distance that have a homogeneous chemical composition. Unfortunately, of the  $\approx 1700$  known OC (e.g. Dias et al., 2002), only  $\approx 140$  possess some metallicity determination, mostly obtained from photometric indicators, such as Washington or Strömgren photometry (see Twarog et al., 1997; Chen et al., 2003, and references therein) and low-resolution spectroscopy (e.g. Friel & Janes, 1993; Friel et al., 2002).

The most accurate way to determine the chemical abundances is to analyse high-resolution spectroscopy. It allows us to investigate not only metallicity, but also abundance ratios – with respect to iron or hydrogen – of other chemical species such as  $\alpha$ -elements,  $s$ -process elements, and  $r$ -process elements, which are synthesised in different environments and on differ-

ent timescales (e.g. SNe Ia, SNe II, giants, supergiants, etc). In the past few years, a number of research groups have addressed the challenge of increasing the number of OC with chemical abundances determined from high-resolution spectroscopy (e.g. Sestito et al., 2004; D’Orazi et al., 2006; Sestito et al., 2006; Bragaglia et al., 2008; Pace et al., 2008; D’Orazi et al., 2009; Friel et al., 2010; Pace et al., 2010; Pancino et al., 2010a; Jacobson et al., 2011a). However, the number of OC with chemical abundances determined with this technique is still small (see Section 5), and significant uncertainties remain in the determinations of both the metallicity gradient and the age-metallicity relation, which are the fundamental ingredients of chemical evolution models.

In this paper, the second of a series initiated by Pancino et al. (2010a, hereafter Paper I), we present high quality and homogeneous measurements of chemical abundances for red clump stars in four OC: Be 32, NGC 752, Hyades, and Praesepe. The Hyades is the nearest OC and its four known red giants have been widely studied (Schuler et al., 2009; Mishenina et al., 2007; Fulbright et al., 2007; Schuler et al., 2006; Mishenina et al., 2006; Boyarchuk et al., 2000; Luck & Challener, 1995), hence it provides a very good reference frame to compare our abundances with the literature. Both NGC 752 and Praesepe have been well-studied, but all information about their chemical

<sup>★</sup> Based on observations collected with the fiber spectrograph FOCES at the 2.2m Calar Alto Telescope. Also based on data from 2MASS survey and the WEBDA, VALD, NIST, and GEISA online database.

**Table 1.** Observing logs and programme star properties.

Cluster	Star	$\alpha_{2000}$ (hrs)	$\delta_{2000}$ (deg)	B (mag)	V (mag)	R (mag)	$I^a$ (mag)	$K_S$ (mag)	$n_{exp}$	$t_{exp}^{tot}$ (sec)	$S/N^{tot}$
Be 32 <sup>b</sup>	0456	06:58:08.2	+06:24:19.6	14.76	13.67	—	12.53	11.03	7	18900	60
	1948	06:58:04.2	+06:27:17.1	14.50	13.37	—	12.20	10.68	6	16200	70
NGC 752 <sup>c</sup>	001	01:55:12.6	+37:50:14.6	10.47	9.51	—	—	7.23	4	2400	160
	208	01:57:37.6	+37:39:38.1	10.04	8.97	—	—	6.41	4	2400	180
	213	01:57:38.9	+37:46:12.5	10.08	9.07	—	—	6.68	3	1800	80
	311	01:58:52.9	+37:48:57.3	10.11	9.07	—	—	6.64	4	2400	100
Hyades <sup>d</sup> (Mel 25)	028 ( $\gamma$ tau)	04:19:47.6	+15:37:39.5	4.64	3.65	2.92	2.45	1.52	2	120	560
	041 ( $\delta$ tau)	04:22:56.1	+17:32:33.0	4.75	3.76	3.03	2.56	1.64	3	180	450
	070 ( $\epsilon$ tau)	04:28:37.0	+19:10:49.5	4.55	3.54	2.81	2.31	1.42	3	180	270
Praesepe <sup>e</sup> (NGC 2632) (M 44)	212	08:39:50.7	+19:32:27.0	7.53	6.58	5.87	5.38	4.39	4	240	165
	253	08:40:06.4	+20:00:28.1	7.35	6.38	5.67	5.20	4.20	4	240	215
	283	08:40:22.1	+19:40:11.9	7.42	6.41	5.68	5.21	4.18	2	120	150

<sup>a</sup> All I magnitudes are in the Johnson system ( $I_J$ ) with the exception of those of the Be 32 stars which are in the Cousins system ( $I_C$ ).

<sup>b</sup> Star names from Richtler & Sagar (2001); Coordinates, B, V &  $I_C$  magnitudes from D’Orazi et al. (2006);  $K_S$  magnitudes from 2MASS.

<sup>c</sup> Star names from Heinemann (1926); Coordinates from Høg et al. (2000); B & V magnitudes from Jennens & Helfer (1975);  $K_S$  magnitudes from 2MASS.

<sup>d</sup> Star names from van Bueren (1952); Coordinates from Perryman et al. (1997); B, V, R &  $I_J$  magnitudes from Johnson et al. (1966);  $K_S$  magnitudes from 2MASS.

<sup>e</sup> Star names from Klein Wassink (1927); Coordinates from Perryman et al. (1997); B, V & R magnitudes from Coleman (1982);  $I_J$  magnitudes from Mendoza (1967); Johnson et al. (1966),  $K_S$  magnitudes from 2MASS.

composition is based mainly on their main-sequence stars (e.g. Pace et al., 2008; An et al., 2007; Sestito et al., 2004; Burkhart & Coupry, 1998; Hobbs & Thorburn, 1992). To our knowledge, there have been no recent measurements of the chemical abundance of their giants from high-resolution spectroscopy. Finally, Be 32 has been the subject of some studies (e.g. Richtler & Sagar, 2001; Friel et al., 2010; Bragaglia et al., 2008; D’Orazi et al., 2006). The properties and previous studies of each cluster is described in more depth in Section 4.

This paper is structured as follows: observations and data reduction are described in Section 2; equivalent-width measurements are presented in Section 3, together with the abundance analysis and its uncertainties; results are compared with the literature in Sections 4, 5, and 6; and finally our main conclusions are summarised in Section 7.

## 2. Observational material

A total of twelve stars spread in the four OC were observed. They were selected from the WEBDA<sup>1</sup> database (Mermilliod, 1995), and the 2MASS<sup>2</sup> survey (Cutri et al., 2003; Skrutskie et al., 2006). Table 1 summarizes the identifications, coordinates, and magnitudes of each target star. Their position in the color-magnitude diagram taken from D’Orazi et al. (2006), Johnson (1953), Johnson & Knuckles (1955), and Johnson (1952) for Berkeley 32, NGC 752, Hyades, and Praesepe, respectively, are shown in Figure 1.

Observations were carried out with the fibre echelle spectrograph FOCES (Pfeiffer et al., 1998) attached at the 2.2 m Calar Alto Telescope (Almeria, Spain) between the 1 and 3 of January 2005. The chosen set-up provides a spectral resolution ( $R=\lambda/\delta\lambda$ )

of about 30 000. In summary, all stars were observed in 2–7 exposures lasting 10–30 min each, depending on their magnitudes, until a global signal-to-noise ratio (S/N) of at least 60 per pixel was reached around 6000 Å. Exposures with  $S/N < 20$  were neglected because they were too noisy. Finally, sky exposures as long as our longest exposures (30 min) were taken, but the levels were sufficiently low for us to avoid sky subtraction (as in Paper I). The number of useful exposures, the total integration time, and the global S/N for each star are listed in the last three columns of Table 1.

### 2.1. Data reduction

Various steps of data reduction were performed exactly as in Paper I. Briefly, the frames were de-trended with the IRAF<sup>3</sup> tasks *ccdproc* and *apflatten*. The spectra were then extracted, wavelength-calibrated, normalized, and the echelle orders were merged using tasks in the IRAF *echelle* package. Finally, the noisy ends of each combined spectrum were cut, allowing for an effective wavelength coverage from 5000 to 9000 Å.

Before combining all exposures of each star, we removed sky absorption features (telluric bands of O<sub>2</sub> and H<sub>2</sub>O) with the help of the IRAF task *telluric*. The same two hot, rapidly rotating stars, HR 3982 and HR 8762, of Paper I were used. The strong O<sub>2</sub> band around 7600 Å had been saturated and therefore could not be properly removed. This spectral region was not used for the abundance analysis, in addition to the small gaps between echelle orders that appeared after  $\lambda \approx 8400$  Å.

### 2.2. Radial velocities

We used DAOSPEC (Stetson & Pancino, 2008) to measure the observed radial velocities for each individual exposure with

<sup>1</sup> <http://www.univie.ac.at/webda>

<sup>2</sup> <http://www.ipac.caltech.edu/2mass>. 2MASS (Two Micron All Sky Survey) is a joint project of the University of Massachusetts and the Infrared Processing and Analysis Center/California Institute of Technology, funded by the National Aeronautics and Space Administration and the National Science Foundation.

<sup>3</sup> Image Reduction and Analysis Facility, IRAF is distributed by the National Optical Astronomy Observatories, which are operated by the Association of Universities for Research in Astronomy, Inc., under co-operative agreement with the National Science Foundation.

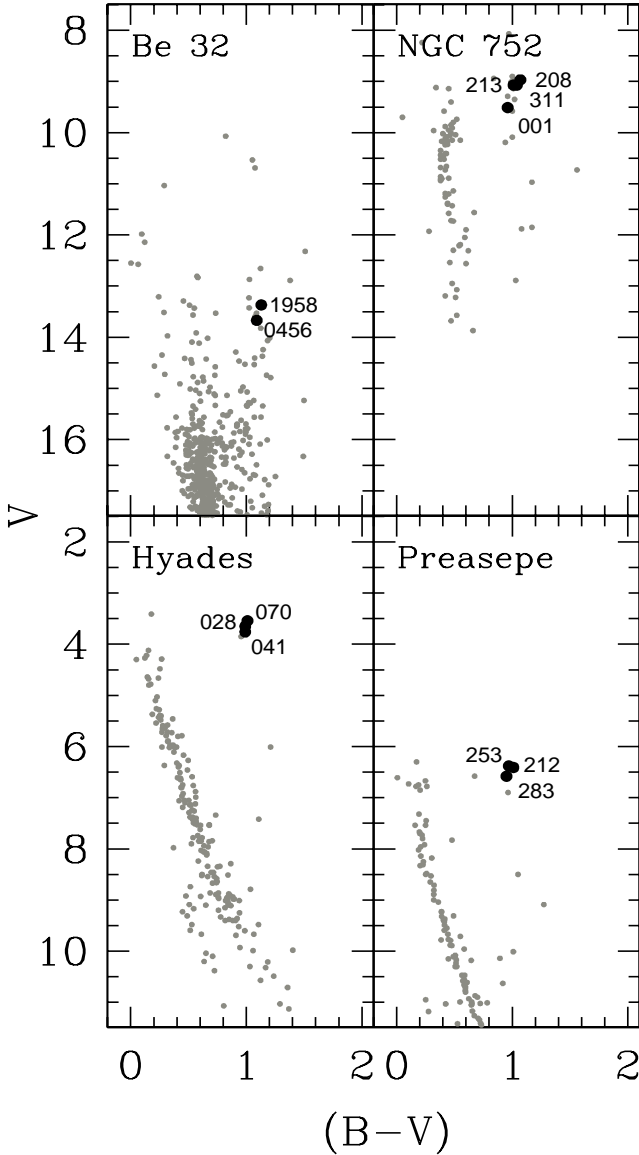


**Fig. 1.** Location of target stars (large black dots with star ID labels) in the color-magnitude diagrams of their respective parent clusters (small grey dots).

$S/N \geq 20$ , using  $\approx 300$  absorption lines of different elements, with typical uncertainties of about  $0.1 \text{ km s}^{-1}$  (see Paper I for details). We used the same linelist as the one used for abundance determinations (see Section 3 for details). Heliocentric corrections were obtained with the IRAF task *rvcorrect*, with a negligible uncertainty of smaller than  $0.005 \text{ km s}^{-1}$ . We also used DAOSPEC to determine the absolute zero-point of the radial velocity determinations, using a list of telluric absorption lines as the input linelist, obtained from the GEISA database (Jacquinet-Husson et al., 1999, 2005). The resulting zero-point corrections, based on  $\approx 250$  telluric lines, are generally no larger than  $\pm 1 \text{ km s}^{-1}$ , with a typical error of about  $\approx 0.5 \text{ km s}^{-1}$ .

The final values, computed as the weighted mean of heliocentric velocities resulting from each exposure of the same star, are listed in Table 2. Our determinations are generally in close agreement with literature values to within  $3\sigma$ , except for star 208 in NGC 752, which has a slightly smaller radial veloc-

**Table 2.** Heliocentric radial velocity measurements and  $1\sigma$  errors ( $V_r \pm \delta V_r$ )<sub>here</sub> for each programme star. Literature measurements are also reported with their uncertainties ( $V_r \pm \delta V_r$ )<sub>lit</sub>.

Cluster	Star	( $V_r \pm \delta V_r$ ) <sub>here</sub> ( $\text{km s}^{-1}$ )	( $V_r \pm \delta V_r$ ) <sub>lit</sub> ( $\text{km s}^{-1}$ )
Be 32 <sup>a</sup>	0456	$105.59 \pm 0.54$	$110.0 \pm 1.2$
	1948	$104.78 \pm 0.35$	$105.5 \pm 4.9$
NGC 752 <sup>b</sup>	001	$5.49 \pm 0.44$	$4.79 \pm 0.15$
	208 <sup>c</sup>	$1.10 \pm 0.23$	$4.86 \pm 0.06$
	213	$5.11 \pm 0.42$	$5.50 \pm 0.10$
	311	$6.00 \pm 0.30$	$5.28 \pm 0.08$
Hyades <sup>d</sup>	028	$38.15 \pm 0.43$	$39.28 \pm 0.12$
	041	$38.56 \pm 0.36$	$39.65 \pm 0.08$
	070	$38.26 \pm 0.35$	$39.37 \pm 0.07$
Praesepe <sup>e</sup> (NGC 2632)	212	$35.96 \pm 0.36$	$34.81 \pm 0.21$
	253	$34.39 \pm 0.27$	$33.67 \pm 0.22$
	283	$34.67 \pm 0.39$	$34.35 \pm 0.20$

<sup>a</sup> D’Orazi et al. (2006).

<sup>b</sup> Mermilliod et al. (1998).

<sup>c</sup> Spectroscopic binary according to Pourbaix et al. (2004).

<sup>d</sup> Griffin et al. (1988).

<sup>e</sup> Famaey et al. (2005).

ity than other objects in this cluster. The fact that this star was recognised as a spectroscopic binary (see Pourbaix et al., 2004; Mermilliod et al., 2007) explains the disagreement. According to its radial velocity curve (Mermilliod et al., 2007), we observed this binary near minimum, which implies that we observed only one of the components of the system. For this reason, and because derived abundances are in good agreement with those of other stars in the same cluster, we retained this object in our final sample. In summary, we considered all the observed targets as likely members of their respective clusters.

### 2.3. Photometric parameters

First guesses of the atmospheric parameters effective temperature ( $T_{\text{eff}}$ ), logarithmic gravity ( $\log g$ ), and microturbulent velocity ( $v_t$ ), for our target stars were derived from a photometric data listed in Table 1, as described in Paper I. In brief,  $T_{\text{eff}}$  were obtained using the Alonso et al. (1999) and Montegriffo et al. (1998) colour-temperature relations, both theoretical and empirical, and the dereddened colours  $(B-V)_0$ ,  $(V-I)_0$ ,  $(V-R)_0$ , and  $(V-K_S)_0$ . We assumed the  $E(B-V)$  values listed in Table 3 and the reddening laws of Cardelli et al. (1989). In the case of Be 32, we have  $I_C$  magnitudes instead of  $I_J$  ones, so we dereddened  $(V-I_C)$  with the law of Dean et al. (1978), and converted it into  $(V-I_J)_0$  with the transformations by Bessell (1979). The  $1\sigma$  errors in each  $T_{\text{eff}}$  estimate were computed using the magnitude and reddening uncertainties together with the standard deviation in the colour-temperature relationships used. The photometric  $T_{\text{eff}}$  estimates, listed in Table 4, are the weighted mean of the different values obtained from each considered colour and colour-temperature relations.

Photometric gravity estimates were derived from the above  $T_{\text{eff}}$  and the bolometric corrections,  $BC_V$ , derived using the Alonso et al. (1999) prescriptions and the fundamental relationships

$$\log \frac{g}{g_\odot} = \log \frac{M}{M_\odot} + 2 \log \frac{R_\odot}{R},$$

**Table 3.** Adopted cluster parameters. When more than one determination exists, the average is shown with  $1\sigma$  errors.

Cluster	E(B-V) (mag)	(m-M) <sub>0</sub> (mag)	Age (Gyr)
Be 32 <sup>a</sup>	0.15±0.05	12.62±0.18	4.8±1.5
NGC 752 <sup>b</sup>	0.038±0.002	8.04±0.23	1.59±0.45
Hyades	≤0.001 <sup>c</sup>	3.34±0.01 <sup>d</sup>	0.70±0.07 <sup>e</sup>
Praesepe	0.027±0.004 <sup>c</sup>	6.22±0.02 <sup>f</sup>	0.65 <sup>g</sup> ±0.25

<sup>a</sup> Averages of measurements by Kaluzny & Mazur (1991), Carraro & Chiosi (1994), Dutra & Bica (2000), Richtler & Sagar (2001), Tadross (2001), Lata et al. (2002), Salaris et al. (2004), D’Orazi et al. (2006), and Tosi et al. (2007).

<sup>b</sup> Averages of measurements by Johnson (1953), Roman (1955), Johnson (1961), Rohlfs & Vanysek (1962), Arp (1962), Eggen (1963), Crawford & Barnes (1970), Patenaude (1978), Hardy (1979), Nicolet (1981), Twarog (1983), Barry et al. (1987), Nissen (1988), Mazzei & Pigatto (1988), Eggen (1989), Francic (1989), Boesgaard (1991), Dzervitis & Paupers (1993), Carraro et al. (1993), Meynet et al. (1993), Daniel et al. (1994), Piatti et al. (1995), Dinescu et al. (1995), Milone et al. (1995), Claria et al. (1996), Dutra & Bica (2000), Loktin & Beshenov (2001), Blake (2002), Blake & Rucinski (2004), Salaris et al. (2004), Bartašič et al. (2007), Taylor (2007), and Giardino et al. (2008).

<sup>c</sup> Derived by Taylor (2006) from a review of published values.

<sup>d</sup> Averages of measurements obtained from the Hipparcos parallaxes by Pinsonneault et al. (1998), Perryman et al. (1998), Narayanan & Gould (1999), Loktin & Beshenov (2001), and Percival et al. (2003).

<sup>e</sup> Averages of measurements by Eggen (1998), Loktin & Beshenov (2001), Salaris et al. (2004), Jameson et al. (2008), and Bouvier et al. (2008).

<sup>f</sup> Averages of measurements obtained from the Hipparcos parallaxes by Pinsonneault et al. (1998), Perryman et al. (1998), van Leeuwen (1999), Loktin (2000), Loktin & Beshenov (2001), and Percival et al. (2003).

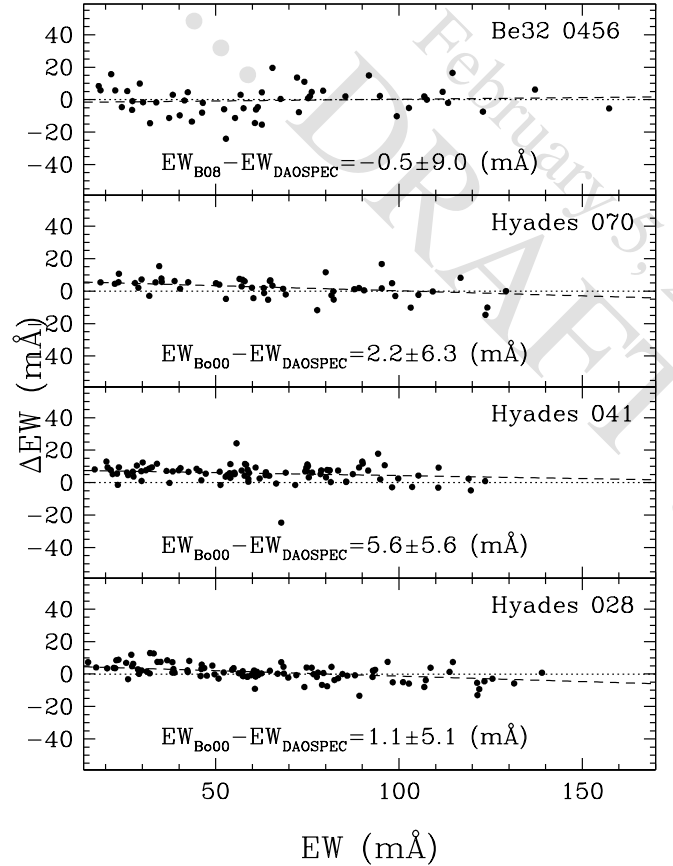
<sup>g</sup> Averages of measurements obtained from the Hipparcos parallaxes by van den Heuvel (1969), Maeder (1971), Mathieu & Mazeh (1988), Mazzei & Pigatto (1988), Boesgaard (1989), Tsvetkov (1993), Piatti et al. (1995), Claria et al. (1996), Hernandez et al. (1998), Loktin & Beshenov (2001), Salaris et al. (2004), Kraus & Hillenbrand (2007), and Gáspár et al. (2009).

$$0.4(M_{\text{bol}} - M_{\text{bol},\odot}) = -4 \log \frac{T_{\text{eff}}}{T_{\text{eff},\odot}} + 2 \log \frac{R_{\odot}}{R},$$

where red clump masses, listed in the last column of Table 4, were extrapolated from Table 1 of Girardi & Salaris (2001). We assumed that  $\log g_{\odot} = 4.437$ ,  $T_{\text{eff},\odot} = 5770$  K and  $M_{\text{bol},\odot} = 4.75$ , in conformity with the IAU recommendations (Andersen, 1999). As above, we averaged all our estimates to obtain  $\log g^{(\text{phot})}$ , listed in column 5 of Table 4.

As discussed in Paper I, the photometric estimate of the microturbulent velocity,  $v_t$ , was obtained using the prescriptions both of Ramírez & Cohen (2003),  $v_t = 4.08 - 5.01 \cdot 10^{-4} T_{\text{eff}}$ , and of Carretta et al. (2004),  $v_t = 1.5 - 0.13 \log g$ . The latter velocity, which takes into account the effect described by Magain (1984)<sup>4</sup>, is on average lower by  $\Delta v_t = 0.50 \pm 0.03$  km s<sup>-1</sup> than the Ramírez & Cohen (2003) estimate. Therefore, we chose not to average the two estimates, but to use them as an indication of the  $v_t$  range to explore in our abundance analysis (see Section 3.2).

<sup>4</sup> However, see the discussion by Mucciarelli (2011) about the pros and cons of the Magain (1984) correction, which depends heavily on data quality and line selection effects.

**Fig. 2.** Comparison of our EW measurements with those by Bragaglia et al. (2008) for star 0456 in Be 32, and by Boyarchuk et al. (2000) for three Hyades giants. Dotted lines mark perfect agreement (zero difference), while dashed lines are linear fits to the data.

### 3. Equivalent widths and abundance analysis

We used the same linelist as that described in Paper I. In brief, all lines and their atomic data were extracted from the VALD database (Kupka et al., 1999), with a few exceptions (see Paper I for details). Briefly, for some highly discrepant Mg lines, we used the NIST  $\log g f$  values; we used the Johansson et al. (2003)  $\log g f$  for the Ni line that contaminates the [O I] line at 6300 Å, and provides oxygen abundances more in line with the other  $\alpha$ -elements; we used the Nd  $\log g f$  values by Den Hartog et al. (2003), which minimize the spread in the Nd abundance. Finally, we tried both the VALD and the NIST values for Ca, finding an average difference of 0.17 dex (see paper I). There is no special reason for choosing NIST over VALD (or vice-versa), so we kept the VALD values to help maintain some homogeneity, but we note that the Ca  $\log g f$  values carry a large uncertainty of the order of 0.2 dex.

#### 3.1. Equivalent widths with DAOSPEC

The task DAOSPEC (Stetson & Pancino, 2008) was used to automatically find and measure equivalent widths (hereafter EW), by performing a Gaussian fitting of the identified lines. DAOSPEC provides a formal error in the Gaussian fit,  $\delta EW$ , and a quality parameter,  $Q$  (see Stetson & Pancino, 2008, and Paper I, for more details). The relative error  $\delta EW/EW$  and the



**Table 4.** Stellar atmosphere parameters for the programme stars (see text).

Cluster	Star	$T_{\text{eff}}^{(phot)}$ (K)	$T_{\text{eff}}^{(spec)}$ (K)	$\log g^{(phot)}$ (cgs)	$\log g^{(spec)}$ (cgs)	$v_t^{(phot)}$ (km s <sup>-1</sup> )	$v_t^{(spec)}$ (km s <sup>-1</sup> )	$M_{\text{clump}}$ ( $M_{\odot}$ )
Be 32	0456	4759±92	4650	2.61±0.14	2.1	1.70±0.30/1.16±0.10	1.4	1.2±0.1
	1948	4706±99	4700	2.47±0.14	2.3	1.72±0.30/1.18±0.10	1.5	1.2±0.1
NGC 752	001	4949±80	5050	3.02±0.14	3.1	1.60±0.30/1.11±0.10	1.3	1.9±0.2
	208	4698±110	4600	2.73±0.14	2.9	1.73±0.31/1.15±0.10	1.2	1.9±0.2
	213	4841±86	4900	2.81±0.14	3.0	1.65±0.30/1.13±0.10	1.4	1.9±0.2
	311	4793±74	4800	2.80±0.14	3.2	1.68±0.30/1.14±0.10	1.2	1.9±0.2
Hyades	028	4865±73	4750	2.67±0.04	2.7	1.64±0.30/1.15±0.15	1.4	2.5±0.1
	041	4871±79	4800	2.71±0.05	2.8	1.64±0.30/1.15±0.15	1.4	2.5±0.1
	070	4858±95	4800	2.62±0.05	2.8	1.65±0.30/1.16±0.15	1.6	2.5±0.1
Praesepe	212	4901±35	4900	2.70±0.07	2.8	1.62±0.30/1.15±0.14	1.5	2.6±0.3
	253	4869±23	4900	2.60±0.07	2.8	1.64±0.30/1.16±0.14	1.6	2.6±0.3
	283	4841±29	4800	2.61±0.07	2.9	1.65±0.30/1.16±0.14	1.4	2.6±0.3

**Table 5.** Equivalent widths and atomic data of the programme stars. The complete version of the table is available at the CDS. Here we show a few lines to illustrate its contents.

$\lambda$ (Å)	Elem	$\chi_{\text{ex}}$ (eV)	$\log gf$ (dex)	Be 32–Star 0456			Be 32–Star 1948			...	Praesepe–Star 283		
				EW (mÅ)	$\delta EW$ (mÅ)	Q	EW (mÅ)	$\delta EW$ (mÅ)	Q		EW (mÅ)	$\delta EW$ (mÅ)	Q
6696.79	Al I	4.02	-1.42	16.5	1.9	0.361	25.3	3.9	0.481	...	30.0	5.0	0.585
6698.67	Al I	3.14	-1.65	47.8	2.7	0.432	43.4	2.6	0.501	...	59.2	1.8	0.321
7361.57	Al I	4.02	-0.90	33.8	3.9	0.633	33.2	6.5	0.946	...	52.1	2.1	0.173
7362.30	Al I	4.02	-0.75	48.6	4.3	0.346	39.7	2.9	0.737	...	72.0	6.9	0.797
7835.31	Al I	4.02	-0.65	53.7	3.7	0.393	48.4	3.9	0.611	...	95.8	9.8	1.399
7836.13	Al I	4.02	-0.49	66.0	7.8	1.279	68.4	5.1	0.783	...	94.0	6.0	0.665
8772.86	Al I	4.02	-0.32	...	...	...	...	...	...	...	102.7	8.7	0.748
8773.90	Al I	4.02	-0.16	115.0	8.6	1.151	111.9	8.3	1.111	...	...	...	...
5853.67	BA2	0.60	-1.00	119.7	3.9	1.098	102.0	2.6	0.343	...	122.1	3.4	0.676

quality parameter  $Q$  can be used to distinguish good and bad lines, and they were indeed used to select the highest quality lines for the abundance analysis, as described in detail in Paper I. The measured EW for our program stars are shown in the electronic version of Table 5 along with the  $\delta EW$  and  $Q$  parameter estimated by DAOSPEC.

Four of our target stars have published EW measurements from high-resolution spectra. These consist of three stars (namely, 028, 041, and 070) observed in the Hyades by Boyarchuk et al. (2000) with  $R \sim 45000$ , and star 0456 in Be 32 studied by Bragaglia et al. (2008) with  $R \sim 40000$ . We have a total of 100, 92, and 51 lines in common for stars 028, 041, and 070 in the Hyades, respectively, and 51 lines for star 0456 in Be 32. Figure 2 compares the comparison between the EW determined with DAOSPEC with the values published by Bragaglia et al. (2008) and Boyarchuk et al. (2000). The differences (see Figure 2) are negligible within the uncertainties; we find a small offset of 5.6 mÅ in the case of star 041 in the Hyades, which is however still within  $1\sigma$ . We can therefore consider our measurements in good agreement with similar studies.

### 3.2. Abundance analysis

Abundance calculations and spectral synthesis (for oxygen) were performed using the latest version of the abundance calculation code originally described by Spite (1967). We used the MARCS model atmospheres developed by Edvardsson et al. (1993). We also used of ABOMAN, a tool developed by E. Rossetti at the INAF, Bologna Observatory, Italy, which allows the semi-automatic processing of data for several objects, using the aforementioned abundance calculation code. The tool

ABOMAN performs all the steps needed to choose the best-fit model automatically (see below) and compute abundance ratios for all elements, and provides all the graphical tools required to analyse the results.

The detailed procedure followed to derive the chemical abundances is described in depth in Paper I. In brief, we calculated Fe I and Fe II abundances for a set of models with parameters extending  $\pm 3\sigma$  around the photometric estimates of Table 4. We chose the model that satisfied simultaneously the following conditions: (i) the abundance of Fe I lines should not vary with excitation potential  $\chi_{\text{ex}}$ ; (ii) the abundance of Fe I lines should not vary significantly with EW, i.e., strong and weak lines should infer the same abundance<sup>5</sup>; (iii) the abundance of Fe I lines should not differ significantly from the abundance of Fe II lines; and (iv) the abundance of Fe I lines should not vary significantly with wavelength.

Once the best-fit model has been found, abundance ratios of all the measured elements were determined, as shown in Table 6, as the average of abundances given by single lines. The internal (random) errors were then computed as  $\sigma / \sqrt{n_{\text{lines}}}$ . Oxygen abundances were determined by means of spectral synthesis of the region around the [O I] forbidden line at 6300 Å. In this case, the internal uncertainty was estimated using the average abundance difference between the best-fit spectrum and two spectra placed approximately  $1\sigma$  (of the Poissonian noise) above and below it. Average cluster abundances (Tables 7) were computed as weighted averages of abundance ratios of single stars.

<sup>5</sup> We decided not to use the Magain (1984) effect, because we prefer to have internally consistent abundances from each line, and because of the additional effects described by Mucciarelli (2011).

**Table 6.** Abundance ratios for single cluster stars, with their internal and external (last column) uncertainties.

Ratio	Berkeley 32		NGC 752				External Uncertainty
	Star 456	Star 1948	Star 001	Star 208	Star 213	Star 311	
[Fe/H]	-0.33±0.02	-0.27±0.02	+0.07±0.01	+0.07±0.01	+0.04±0.01	+0.14±0.01	±0.03
[FeII/H]	-0.30±0.06	-0.29±0.06	+0.02±0.03	+0.06±0.03	+0.05±0.04	+0.18±0.12	±0.03
[ $\alpha$ /Fe]	-0.29±0.21	-0.25±0.09	+0.07±0.04	+0.05±0.12	+0.07±0.12	+0.14±0.09	±0.07
[Al/Fe]	+0.15±0.06	+0.08±0.07	-0.11±0.04	-0.12±0.03	-0.06±0.06	-0.21±0.06	±0.05
[Ba/Fe]	+0.52±0.05	+0.35±0.17	+0.55±0.04	+0.52±0.04	+0.51±0.01	+0.57±0.06	±0.04
[Ca/Fe]	-0.06±0.08	-0.05±0.04	-0.02±0.03	-0.12±0.02	-0.09±0.03	-0.17±0.05	±0.06
[Co/Fe]	+0.02±0.05	+0.09±0.04	-0.03±0.03	+0.06±0.04	+0.00±0.03	+0.05±0.05	±0.04
[Cr/Fe]	-0.25±0.07	+0.04±0.07	+0.02±0.03	+0.00±0.03	-0.01±0.03	-0.01±0.04	±0.05
[La/Fe]	-0.14±0.02	-0.04±0.08	+0.14±0.06	+0.18±0.03	+0.18±0.09	+0.32±0.13	±0.04
[Mg/Fe]	+0.38±0.12	+0.24±0.16	+0.13±0.06	+0.16±0.05	+0.20±0.04	+0.06±0.03	±0.09
[Na/Fe]	-0.14±0.08	-0.08±0.10	+0.05±0.01	-0.07±0.02	-0.03±0.05	-0.10±0.05	±0.04
[Nd/Fe]	-0.05±0.13	+0.04±0.03	+0.29±0.14	+0.27±0.23	+0.34±0.11	+0.46±0.18	±0.13
[Ni/Fe]	-0.04±0.03	-0.01±0.03	-0.04±0.02	+0.00±0.02	-0.02±0.02	+0.03±0.03	±0.02
[O/Fe]	-0.16±0.13	+0.15±0.11	+0.15±0.06	-0.06±0.05	+0.02±0.08	+0.00±0.06	±0.08
[Sc/Fe]	+0.02±0.05	-0.02±0.05	-0.02±0.05	+0.04±0.06	+0.05±0.06	+0.09±0.08	±0.05
[Si/Fe]	+0.18±0.04	+0.11±0.04	-0.03±0.03	+0.04±0.03	+0.04±0.03	+0.01±0.04	±0.04
[TiI/Fe]	-0.10±0.05	-0.04±0.05	+0.00±0.02	-0.03±0.02	-0.08±0.02	-0.13±0.03	±0.03
[TiII/Fe]	-0.17±0.05	+0.01±0.07	+0.03±0.02	+0.08±0.07	+0.07±0.06	+0.15±0.13	±0.03
[V/Fe]	-0.14±0.10	-0.07±0.05	+0.00±0.02	+0.16±0.05	-0.04±0.03	+0.05±0.06	±0.06
[Y/Fe]	-0.41±N.A.	-0.09±N.A.	-0.12±0.06	-0.03±0.10	+0.03±0.07	+0.05±0.09	±0.04

Ratio	Hyades (Mel 25)			Praesepe (NGC 2632)			External Uncertainty
	Star 28	Star 41	Star 70	Star 212	Star 253	Star 283	
[Fe/H]	+0.12±0.01	+0.10±0.01	+0.11±0.01	+0.11±0.01	+0.18±0.01	+0.21±0.01	±0.03
[FeII/H]	+0.13±0.03	+0.13±0.03	+0.09±0.03	+0.10±0.03	+0.16±0.03	+0.23±0.04	±0.03
[ $\alpha$ /Fe]	+0.13±0.15	+0.11±0.12	+0.09±0.11	+0.11±0.15	+0.18±0.14	+0.19±0.13	±0.07
[Al/Fe]	-0.01±0.05	+0.00±0.05	+0.02±0.05	+0.01±0.04	+0.02±0.06	-0.04±0.05	±0.05
[Ba/Fe]	+0.37±0.05	+0.39±0.05	+0.31±0.05	+0.30±0.08	+0.27±0.06	+0.37±0.05	±0.04
[Ca/Fe]	-0.07±0.03	-0.06±0.03	-0.07±0.02	-0.07±0.02	-0.08±0.03	-0.11±0.03	±0.06
[Co/Fe]	+0.00±0.04	+0.01±0.03	+0.06±0.03	+0.05±0.03	+0.01±0.03	+0.05±0.05	±0.04
[Cr/Fe]	+0.02±0.03	+0.03±0.03	+0.08±0.04	+0.06±0.03	+0.04±0.04	+0.04±0.04	±0.05
[La/Fe]	-0.12±0.06	-0.08±0.05	-0.05±0.05	-0.07±0.05	-0.04±0.05	-0.04±0.04	±0.04
[Mg/Fe]	+0.13±0.05	+0.06±0.04	+0.21±0.07	+0.31±0.06	+0.27±0.05	+0.22±0.06	±0.09
[Na/Fe]	+0.19±0.02	+0.18±0.02	+0.18±0.02	+0.23±0.02	+0.30±0.03	+0.18±0.05	±0.04
[Nd/Fe]	+0.04±0.29	+0.08±0.30	+0.08±0.28	+0.00±0.21	+0.05±0.25	+0.10±0.31	±0.13
[Ni/Fe]	+0.02±0.02	+0.04±0.02	+0.03±0.02	+0.01±0.02	+0.01±0.02	+0.04±0.03	±0.02
[O/Fe]	-0.35±0.07	-0.25±0.05	-0.22±0.07	-0.11±0.09	-0.14±0.07	-0.09±0.06	±0.08
[Sc/Fe]	-0.04±0.05	+0.00±0.05	-0.02±0.06	-0.10±0.06	+0.03±0.05	+0.00±0.06	±0.05
[Si/Fe]	+0.09±0.03	+0.09±0.02	+0.10±0.03	+0.06±0.03	+0.07±0.03	+0.04±0.03	±0.04
[TiI/Fe]	-0.12±0.02	-0.11±0.02	-0.06±0.02	-0.05±0.03	-0.08±0.02	-0.09±0.02	±0.03
[TiII/Fe]	-0.03±0.06	+0.00±0.07	-0.02±0.11	-0.05±0.10	-0.02±0.08	+0.05±0.08	±0.03
[V/Fe]	+0.02±0.04	+0.00±0.03	+0.09±0.03	+0.06±0.04	+0.04±0.03	+0.10±0.04	±0.06
[Y/Fe]	-0.12±0.05	-0.06±0.06	-0.07±0.05	-0.11±0.10	-0.12±0.07	-0.11±0.09	±0.04

Comparison of our results with available literature is discussed in details in Section 4.

### 3.3. Abundance uncertainties and the Sun

The internal (random) uncertainty described above includes uncertainties related to the measurement of EW and to the atomic parameters (dominated by  $\log gf$  determinations). We must consider other sources of uncertainty (see Paper I for details) such as: the uncertainty owing to the choice of atmospheric parameters; the uncertainty owing to the continuum normalization procedure; the uncertainty in the reference solar abundance values.

Uncertainties due to the choice of stellar parameters were evaluated with the method proposed by Cayrel et al. (2004). In brief, we altered the predominant atmospheric parameter, i.e., by altering one atmospheric parameter,  $T_{\text{eff}}$ , within its uncertainty ( $\sim 100$  K) and re-optimizing the other parameters for the hottest and coolest stars in our sample. We re-calculated abundances with the procedure described in the previous Section. The exter-

nal uncertainties, listed in the last column of Table 6, are estimated by averaging errors calculated with the higher and lower temperatures for the warmest and coolest stars in our sample (namely, stars 001 and 208 in NGC 752).

Uncertainties due to the continuum normalization procedure might also affect the obtained EW and, therefore, the derived abundances. Their contribution is estimated by averaging the differences between the EW obtained with the “best-fit” continuum and those derived by lowering and raising the continuum level by the continuum placement uncertainty. This is calculated from Equation 7 of Stetson & Pancino (2008). The typical uncertainty caused by the continuum placement is  $\Delta EW \sim 1$  mÅ and almost independent of the EW. This small uncertainty has a negligible impact on the derived abundances in comparison with other sources of uncertainty described above. Therefore, they have not been explicitly included in the error budget.

To validate the whole procedure used here, in Paper I we performed an abundance analysis of the ESO HARPS solar spectrum reflected by Ganymede. We used the same line list, model

**Table 7.** Average cluster abundances, obtained as the weighted average of the single stars abundances in each of them.

Ratio	Be 32	NGC 752	Hyades	Praesepe (M 44)
[Fe/H]	$-0.30 \pm 0.02 (\pm 0.03)$	$+0.08 \pm 0.04 (\pm 0.03)$	$+0.11 \pm 0.01 (\pm 0.03)$	$+0.16 \pm 0.05 (\pm 0.03)$
[ $\alpha$ /Fe]	$-0.04 \pm 0.14 (\pm 0.07)$	$+0.02 \pm 0.06 (\pm 0.07)$	$+0.00 \pm 0.12 (\pm 0.07)$	$+0.00 \pm 0.14 (\pm 0.07)$
[Al/Fe]	$+0.12 \pm 0.05 (\pm 0.05)$	$-0.12 \pm 0.06 (\pm 0.05)$	$+0.00 \pm 0.02 (\pm 0.05)$	$+0.00 \pm 0.03 (\pm 0.05)$
[Ba/Fe]	$+0.51 \pm 0.12 (\pm 0.04)$	$+0.52 \pm 0.03 (\pm 0.04)$	$+0.36 \pm 0.04 (\pm 0.04)$	$+0.33 \pm 0.05 (\pm 0.04)$
[Ca/Fe]	$-0.05 \pm 0.01 (\pm 0.06)$	$-0.09 \pm 0.06 (\pm 0.06)$	$-0.07 \pm 0.01 (\pm 0.06)$	$-0.08 \pm 0.02 (\pm 0.06)$
[Co/Fe]	$+0.07 \pm 0.05 (\pm 0.04)$	$+0.01 \pm 0.04 (\pm 0.04)$	$+0.03 \pm 0.03 (\pm 0.04)$	$+0.04 \pm 0.02 (\pm 0.04)$
[Cr/Fe]	$-0.11 \pm 0.21 (\pm 0.05)$	$+0.00 \pm 0.01 (\pm 0.05)$	$+0.04 \pm 0.03 (\pm 0.05)$	$+0.05 \pm 0.01 (\pm 0.05)$
[La/Fe]	$-0.14 \pm 0.07 (\pm 0.04)$	$+0.18 \pm 0.08 (\pm 0.04)$	$-0.08 \pm 0.04 (\pm 0.04)$	$-0.05 \pm 0.02 (\pm 0.04)$
[Mg/Fe]	$+0.33 \pm 0.10 (\pm 0.09)$	$+0.12 \pm 0.06 (\pm 0.09)$	$+0.10 \pm 0.08 (\pm 0.09)$	$+0.27 \pm 0.05 (\pm 0.09)$
[Na/Fe]	$-0.12 \pm 0.04 (\pm 0.04)$	$+0.01 \pm 0.07 (\pm 0.04)$	$+0.18 \pm 0.01 (\pm 0.04)$	$+0.25 \pm 0.06 (\pm 0.04)$
[Nd/Fe]	$+0.03 \pm 0.06 (\pm 0.13)$	$+0.34 \pm 0.09 (\pm 0.13)$	$+0.07 \pm 0.02 (\pm 0.13)$	$+0.04 \pm 0.05 (\pm 0.13)$
[Ni/Fe]	$-0.03 \pm 0.02 (\pm 0.02)$	$-0.01 \pm 0.03 (\pm 0.02)$	$+0.03 \pm 0.01 (\pm 0.02)$	$+0.02 \pm 0.02 (\pm 0.02)$
[O/Fe]	$+0.00 \pm 0.16 (\pm 0.08)$	$+0.03 \pm 0.04 (\pm 0.08)$	$-0.27 \pm 0.04 (\pm 0.08)$	$-0.11 \pm 0.03 (\pm 0.08)$
[Sc/Fe]	$+0.00 \pm 0.03 (\pm 0.05)$	$+0.03 \pm 0.05 (\pm 0.05)$	$-0.02 \pm 0.02 (\pm 0.05)$	$-0.04 \pm 0.05 (\pm 0.05)$
[Si/Fe]	$+0.14 \pm 0.05 (\pm 0.04)$	$+0.02 \pm 0.03 (\pm 0.04)$	$+0.09 \pm 0.01 (\pm 0.04)$	$+0.06 \pm 0.02 (\pm 0.04)$
[Ti/Fe]	$-0.08 \pm 0.07 (\pm 0.03)$	$-0.03 \pm 0.06 (\pm 0.03)$	$-0.09 \pm 0.04 (\pm 0.03)$	$-0.07 \pm 0.03 (\pm 0.07)$
[V/Fe]	$-0.08 \pm 0.05 (\pm 0.06)$	$+0.01 \pm 0.09 (\pm 0.06)$	$+0.04 \pm 0.05 (\pm 0.06)$	$+0.06 \pm 0.03 (\pm 0.06)$
[Y/Fe]	$-0.23 \pm 0.23 (\pm 0.04)$	$-0.03 \pm 0.08 (\pm 0.04)$	$-0.09 \pm 0.03 (\pm 0.04)$	$-0.11 \pm 0.01 (\pm 0.04)$

**Table 8.** High-resolution average Be 32 abundances.

	<i>Here</i>	F10 <sup>a</sup>	B08 <sup>b</sup>
R= $\lambda/\delta\lambda$	30000	28000	40000
S/N	50–100	100	45–100
[Fe/H]	$-0.30 \pm 0.02$	$-0.30 \pm 0.02$	$-0.29 \pm 0.04$
[Al/Fe]	$+0.12 \pm 0.05$	$+0.19 \pm 0.06$	$+0.11 \pm 0.10$
[Ba/Fe]	$+0.51 \pm 0.12$	—	$+0.29 \pm 0.10$
[Ca/Fe]	$-0.05 \pm 0.01$	$-0.07 \pm 0.01$	$+0.07 \pm 0.04$
[Co/Fe]	$+0.07 \pm 0.05$	$+0.00 \pm 0.01$	—
[Cr/Fe]	$-0.11 \pm 0.21$	$-0.16 \pm 0.11$	$-0.05 \pm 0.04$
[La/Fe]	$-0.14 \pm 0.07$	—	—
[Mg/Fe]	$+0.33 \pm 0.10$	$+0.13 \pm 0.01$	$+0.27 \pm 0.08$
[Na/Fe]	$-0.12 \pm 0.04$	$+0.20 \pm 0.01$	$+0.13 \pm 0.02$
[Ni/Fe]	$-0.03 \pm 0.02$	$-0.02 \pm 0.01$	$+0.00 \pm 0.04$
[O/Fe]	$+0.00 \pm 0.16$	$-0.01 \pm 0.03$	—
[Sc/Fe]	$+0.00 \pm 0.03$	—	—
[Si/Fe]	$+0.14 \pm 0.05$	$+0.27 \pm 0.05$	$+0.12 \pm 0.04$
[Ti/Fe]	$-0.08 \pm 0.07$	$-0.17 \pm 0.01$	$+0.11 \pm 0.06$
[V/Fe]	$-0.08 \pm 0.05$	—	—
[Y/Fe]	$-0.23 \pm 0.23$	—	—

<sup>a</sup> Friel et al. (2010), from 2 stars.<sup>b</sup> Bragaglia et al. (2008) and Sestito et al. (2006), from 10 red clump and RGB stars.

atmospheres, and abundance calculation code that we used on our OC target stars, and found solar values for all elements, with the only marginal exceptions of barium and aluminium (see also Section 5). While the details of this analysis can be found in Paper I, we mention here that our reference solar abundances are taken from Grevesse et al. (1996).

## 4. Cluster-by-cluster discussion

### 4.1. Berkeley 32

Berkeley 32 ( $\alpha_{2000} = 06^h58^m07^s$  and  $\delta_{2000} = +06^\circ25'43''$ ) is a distant OC ( $R_{gc}=11.6$  kpc) located towards the Galactic anticentre and situated 260 pc above the disc plane. Its distance makes it one of the crucial clusters for a correct determination of the metallicity gradient along the Galactic disc, and therefore one of the key OC to the understanding of disc formation and evolution. The color-magnitude diagram of this cluster

(e.g. D’Orazi et al., 2006), contaminated by disc stars, shows a clear main sequence turn-off with a sparsely populated red giant branch. Determinations of its age, mainly using morphological indicators, yield a value of  $\approx 5$  Gyr (e.g. D’Orazi et al., 2006; Salaris et al., 2004; Richtler & Sagar, 2001; Carraro & Chiosi, 1994; Kaluzny & Mazur, 1991).

Given its large distance, it has not been well-studied spectroscopically, but we could compare our results with two recent high-resolution studies of Bragaglia et al. (2008) and Friel et al. (2010). We found a very close agreement of our abundance ratios with those studies (see Table 8). The exceptions are Ba and Na. It is well-known that Ba abundances are enhanced by HFS (e.g. D’Orazi et al., 2009) effects that should explain the differences from Bragaglia et al. (2008). The [Na/Fe] ratio is lower than the values reported by Bragaglia et al. (2008) and Friel et al. (2010) by  $-0.25$  and  $-0.32$  dex, respectively. The difficulty in measuring Na lines, which suffer from NLTE effects, could easily explain this controversy. Moreover, different model atmospheres, stellar and atomic parameters, etc., between different studies may also play a role (and remove this discrepancy).

### 4.2. NGC 752

NGC 752 ( $\alpha_{2000} = 01^h57^m41^s$ ,  $\delta_{2000} = +37^\circ47'06''$ ) is an old ( $\sim 1.6$  Gyr) OC located in the solar neighbourhood at a distance of  $\approx 400$  pc. This cluster has a low central concentration and contains a relatively small number of members. Its color-magnitude diagram (e.g. Johnson, 1953) has a still poorly understood morphology. The turn-off area is well-populated by early F-type stars, while the low main-sequence appears to be sparsely populated (Figure 1). This, together with the age of this cluster, may be an indication of the dynamic escape of low mass stars. Stellar evolution models also predict a well-populated red giant branch, which is not observed. All the known red giants are located in the red clump region (Bartašiūtė et al., 2007), which has a peculiar morphology because it has a faint extension slightly to the blue of its main concentration, which cannot be reproduced by stellar evolution models (Girardi et al., 2000).

Photometry and low/medium resolution spectroscopy studies (see Bartašiūtė et al., 2007, and references therein) determined a slightly subsolar metallicity (i.e. [Fe/H] =  $-0.16 \pm 0.05$ , Friel & Janes, 1993). A similar result was found with high-

**Table 9.** Abundance comparison of individual Hyades stars (see text).

Parameter	Here	S09/S06	M07/M06	F07	Bo00	LC95
Resolution	30000	60000	42000	30000	45000	30000
S/N	300–600	~500	100–350	175	100–300	>100
Star	028 ( $\gamma$ tau)					
$T_{eff}$ (K)	4750	4965	4955	4823	4956	4900
$\log g$ (dex)	2.7	2.63	2.7	2.43	2.83	2.6
$v_t$ (km s <sup>-1</sup> )	1.4	1.32	1.4	1.57	1.35	2.0
[FeI/H]	+0.12±0.01	+0.14±0.08	+0.11	+0.16±0.05	+0.11±0.01	+0.13±0.02
[FeII/H]	+0.13±0.03	+0.22±0.16	+0.10	+0.09±0.08	+0.11±0.02	+0.12±0.02
[Al/Fe]	-0.01±0.05	+0.20±0.01	—	+0.19±0.07	+0.12±0.00	-0.17±0.03
[Ba/Fe]	+0.37±0.05	—	-0.07	—	+0.09±0.05	-0.04±0.00
[Ca/Fe]	-0.07±0.03	—	+0.10±0.12	-0.01±0.11	+0.01±0.04	-0.28±0.04
[Co/Fe]	+0.00±0.04	—	—	—	+0.02±0.02	+0.04±0.04
[Cr/Fe]	+0.02±0.03	—	—	—	-0.01±0.02	-0.03±0.11
[La/Fe]	-0.12±0.06	—	-0.23	—	-0.03±0.02	—
[Mg/Fe]	+0.13±0.05	+0.43±0.01	-0.08	+0.03±0.07	+0.16±0.02	+0.18±0.05
[Na/Fe]	+0.19±0.02	+0.49±0.05	+0.22	+0.05±0.11	+0.32±0.01	+0.22±0.05
[Nd/Fe]	+0.04±0.29	—	-0.15	—	-0.02±0.03	+0.07±0.00
[Ni/Fe]	+0.02±0.02	+0.12±0.07	-0.04±0.12	—	+0.00±0.03	+0.06±0.03
[O/Fe]	-0.35±0.07	-0.09±0.06	-0.09	-0.04±0.11	—	—
[Sc/Fe]	-0.04±0.05	—	—	—	+0.00±0.02	+0.01±0.08
[Si/Fe]	+0.09±0.03	—	+0.07±0.12	+0.09±0.09	+0.09±0.03	+0.21±0.03
[TiI/Fe]	-0.12±0.02	—	—	-0.05±0.10	-0.01±0.01	-0.14±0.03
[TiII/Fe]	-0.03±0.06	—	—	-0.04±0.15	—	—
[V/Fe]	+0.02±0.04	—	—	—	+0.01±0.02	—
[Y/Fe]	-0.12±0.05	—	-0.11	—	+0.01±0.01	+0.10±0.00
Star	041 ( $\delta$ tau)					
$T_{eff}$ (K)	4800	4938	4975	—	4980	4875
$\log g$ (dex)	2.8	2.69	2.65	—	2.83	2.4
$v_t$ (km s <sup>-1</sup> )	1.4	1.40	1.4	—	1.25	2.0
[FeI/H]	+0.10±0.01	+0.14±0.07	+0.11	—	+0.19±0.01	+0.07±0.01
[FeII/H]	+0.13±0.03	+0.26±0.16	+0.07	—	+0.18±0.03	+0.04±0.02
[Al/Fe]	+0.00±0.05	+0.16±0.01	—	—	+0.08±0.01	-0.14±0.01
[Ba/Fe]	+0.39±0.05	—	-0.02	—	+0.15±0.01	-0.13±0.00
[Ca/Fe]	-0.06±0.03	—	+0.08±0.12	—	+0.00±0.05	-0.17±0.06
[Co/Fe]	+0.01±0.03	—	—	—	+0.01±0.03	+0.10±0.05
[Cr/Fe]	+0.03±0.03	—	—	—	-0.04±0.02	-0.06±0.09
[La/Fe]	-0.08±0.05	—	-0.33	—	-0.05±0.09	—
[Mg/Fe]	+0.06±0.04	+0.36±0.02	-0.10	—	+0.15±0.01	+0.33±0.07
[Na/Fe]	+0.18±0.02	+0.44±0.05	+0.16	—	+0.32±0.01	+0.28±0.05
[Nd/Fe]	+0.08±0.30	—	-0.17	—	+0.02±0.02	-0.17±0.00
[Ni/Fe]	+0.04±0.02	-0.03±0.06	+0.06±0.09	—	+0.09±0.06	+0.11±0.03
[O/Fe]	-0.25±0.05	-0.03±0.06	-0.21	—	—	—
[Sc/Fe]	+0.00±0.05	—	—	—	+0.01±0.02	-0.02±0.07
[Si/Fe]	+0.09±0.02	—	+0.07±0.11	—	+0.06±0.02	+0.23±0.03
[TiI/Fe]	-0.11±0.02	—	—	—	-0.04±0.02	-0.07±0.03
[TiII/Fe]	-0.00±0.07	—	—	—	—	—
[V/Fe]	+0.00±0.03	—	—	—	+0.02±0.02	—
[Y/Fe]	-0.06±0.06	—	-0.10	—	-0.04±0.03	+0.19±0.00
Star	070 ( $\epsilon$ tau)					
$T_{eff}$ (K)	4800	4911	4925	4838	4880	—
$\log g$ (dex)	2.8	2.57	2.55	2.52	2.50	—
$v_t$ (km s <sup>-1</sup> )	1.6	1.47	1.4	1.63	1.46	—
[FeI/H]	+0.11±0.01	+0.20±0.08	+0.11	+0.21±0.07	+0.11±0.01	—
[FeII/H]	+0.09±0.03	+0.22±0.16	+0.11	+0.18±0.10	+0.05±0.03	—
[Al/Fe]	+0.02±0.05	+0.15±0.01	—	+0.17±0.08	+0.20±0.01	—
[Ba/Fe]	+0.31±0.05	—	-0.02	—	+0.09±0.01	—
[Ca/Fe]	-0.07±0.02	—	+0.11±0.12	+0.01±0.10	+0.09±0.03	—
[Co/Fe]	+0.06±0.03	—	—	—	-0.01±0.04	—
[Cr/Fe]	+0.08±0.04	—	—	—	+0.00±0.01	—
[La/Fe]	-0.05±0.05	—	-0.20	—	-0.17±0.00	—
[Mg/Fe]	+0.21±0.07	+0.37±0.02	-0.08	-0.03±0.08	—	—
[Na/Fe]	+0.18±0.02	+0.41±0.04	+0.23	+0.04±0.11	+0.40±0.04	—
[Nd/Fe]	+0.08±0.28	—	-0.21	—	-0.10±0.05	—
[Ni/Fe]	+0.03±0.02	+0.06±0.08	+0.09±0.11	—	+0.00±0.02	—
[O/Fe]	-0.22±0.07	-0.13±0.06	-0.01	-0.04±0.13	—	—
[Sc/Fe]	-0.04±0.05	—	—	—	—	—
[Si/Fe]	+0.10±0.03	—	+0.09±0.11	+0.05±0.11	+0.09±0.03	—
[TiI/Fe]	-0.06±0.01	—	—	-0.01±0.08	-0.05±0.03	—
[TiII/Fe]	-0.02±0.11	—	—	-0.14±0.11	—	—
[V/Fe]	+0.09±0.03	—	—	—	-0.04±0.03	—
[Y/Fe]	-0.07±0.05	—	-0.11	—	-0.05±0.03	—



**Table 10.** High-resolution average Hyades abundances from giants.

	<i>Here</i>	S09/S06 <sup>a</sup>	Bo00 <sup>b</sup>	V99 <sup>c</sup>
R= $\lambda/\delta\lambda$	30000	60000	45000	30–65000
S/N	50–100	100–200	100–300	~200
[Fe/H]	+0.11±0.01	+0.21±0.04	+0.12±0.06	−0.05±0.03
[Al/Fe]	+0.00±0.02	+0.17±0.03	+0.13±0.06	—
[Ba/Fe]	+0.36±0.04	—	+0.10±0.03	−0.03±0.07
[Ca/Fe]	−0.07±0.01	—	+0.03±0.05	+0.03±0.04
[Co/Fe]	+0.03±0.03	—	+0.00±0.02	—
[Cr/Fe]	+0.04±0.03	—	−0.02±0.02	—
[La/Fe]	−0.08±0.04	—	−0.10±0.08	—
[Mg/Fe]	+0.10±0.08	+0.38±0.03	+0.16±0.01	+0.17±0.04
[Na/Fe]	+0.18±0.01	+0.45±0.04	+0.37±0.05	+0.10±0.05
[Ni/Fe]	+0.03±0.01	+0.05±0.07	+0.05±0.06	+0.04±0.04
[O/Fe]	−0.27±0.04	−0.08±0.05	—	+0.11±0.04
[Sc/Fe]	−0.02±0.02	—	+0.00±0.01	+0.03±0.07
[Si/Fe]	+0.09±0.01	—	+0.07±0.01	+0.13±0.03
[Ti/Fe]	−0.09±0.04	—	−0.04±0.02	—
[V/Fe]	+0.04±0.05	—	−0.01±0.03	—
[Y/Fe]	−0.09±0.03	—	−0.04±0.02	−0.04±0.07

<sup>a</sup> Schuler et al. (2009) and Schuler et al. (2006), from the same 3 K giants studied here.

<sup>b</sup> Boyarchuk et al. (2000), from the same 3 K giants studied here.

<sup>c</sup> Varenne & Monier (1999), from 29 F dwarfs.

resolution spectroscopy ( $R \approx 40\,000$ ,  $S/N \approx 80$ –150) in eight F-type stars around the main sequence turn-off ( $[Fe/H] = -0.09 \pm 0.05$ , Hobbs & Thorburn, 1992). However, an investigation based on high-resolution spectroscopy ( $R \approx 57\,000$ ,  $S/N \approx 30$ –80) of 18 G giant stars obtained a solar  $[Fe/H]$  ratio ( $[Fe/H] = +0.01 \pm 0.04$ , Sestito et al., 2004) in closer agreement with the value determined here. To our knowledge, we are the first to publish abundance ratios of elements other than  $[Fe/H]$  for this cluster.

#### 4.3. Hyades

The Hyades cluster (Melotte 25;  $\alpha_{2000} = 04^h 26^m 54^s$  and  $\delta_{2000} = +15^\circ 52' 00''$ ) is the closest OC to the Sun ( $\sim 45$  pc) located in the constellation of Taurus. Its proximity has motivated an extensive study lasting more than a century (starting with Hertzsprung, 1909). The OC is embedded into a moving group with the same name, which suggests that it would be part of a dynamical stream coming from the inner Galaxy or a disrupting cluster (Famaey et al., 2007).

Being one of the most studied clusters, both photometrically and spectroscopically, it is the ideal cluster for abundance analysis comparisons. The color-magnitude diagram of this young OC ( $\sim 0.7$  Gyr, see Table 3; e.g. Johnson & Knuckles, 1955) contains only four red giant stars that have been confirmed as members from their parallaxes, proper motions, and radial velocities. Most of the existing abundance studies are focused on main sequence stars (see e.g. Paulson et al., 2003; Burkhart & Coupry, 2000; Varenne & Monier, 1999, and references therein). A comparison of the Hyades average abundances determined from some (or all) of the known four red giants are shown in Table 10. The averages of the abundances compiled until 1999 by Varenne & Monier (1999) are shown in the last column of Table 10 for reference. In general,  $[Fe/H]$  appears slightly supersolar, while all other abundance ratios are solar, and our abundance ratios agree well with literature values.

**Table 11.** High-resolution average Praesepe (NGC 2632) abundances.

	<i>Here</i>	P08 <sup>a</sup>	A07 <sup>b</sup>	Bu98 <sup>c</sup>
R= $\lambda/\delta\lambda$	30000	100000	55000	90000
S/N	50–100	$\approx 80$	$\approx 100$	~200
[Fe/H]	+0.16±0.05	+0.27±0.10	+0.11±0.03	+0.40±0.14
[Al/Fe]	+0.00±0.03	−0.05±0.12	—	−0.19±0.17
[Ba/Fe]	+0.33±0.05	+0.22±0.06	—	—
[Ca/Fe]	−0.08±0.02	+0.00±0.11	—	+0.04±0.16
[Co/Fe]	+0.04±0.02	—	—	—
[Cr/Fe]	+0.05±0.01	−0.01±0.08	—	—
[La/Fe]	−0.05±0.02	—	—	—
[Mg/Fe]	+0.27±0.05	—	—	—
[Na/Fe]	+0.25±0.06	−0.04±0.12	—	—
[Ni/Fe]	+0.02±0.02	−0.02±0.12	—	+0.21±0.17
[O/Fe]	−0.11±0.03	−0.40±0.20	—	—
[Sc/Fe]	−0.04±0.05	—	—	—
[Si/Fe]	+0.06±0.02	−0.01±0.12	—	—
[Ti/Fe]	−0.07±0.03	−0.04±0.12	—	—
[V/Fe]	+0.06±0.03	—	—	—
[Y/Fe]	−0.11±0.01	—	—	—

<sup>a</sup> Pace et al. (2008), from 6 G and 1 F main sequence stars.

<sup>b</sup> An et al. (2007), from 4 G dwarfs stars.

<sup>c</sup> Burkhart & Coupry (1998), from 10 Am stars.

The three late-type Hyades giants (028, 041, and 070) have been widely studied (e.g. Luck & Challener, 1995; Boyarchuk et al., 2000; Schuler et al., 2006, 2009; Mishenina et al., 2006, 2007; Fulbright et al., 2007). In Table 9 we compiled available literature data. Our temperatures are slightly lower (by  $\sim 100$  K) than the literature ones, whereas our values of  $\log g$  and  $v_t$  are similar. These marginal differences appear to have no significant impact on the derived abundance ratios, which agree very well with literature ones. Exceptions are Al, Ba, and O, which suffer from technical measurement problems (not strictly related to the Hyades cluster) and are discussed in Sections 3.3 and 5.

#### 4.4. Praesepe (NGC 2632)

The cluster popularly known as Praesepe or Beehive (also called M 44, NGC 2632 or Melotte 88;  $\alpha_{2000} = 08^h 40^m 24^s$  and  $\delta_{2000} = +19^\circ 40' 00''$ ), is an old OC (0.65 Gyr, see Table 3) well known from the antiquity. It is located in the Cancer constellation at a distance of  $\approx 175$  pc, computed from Hipparcos parallaxes.

Its metal content was derived with different methods (e.g. Friel & Boesgaard, 1992; Komarov & Basak, 1993; Claria et al., 1996; Hui-Bon-Hoa & Alecian, 1998; Burkhart & Coupry, 1998, 2000; Dias et al., 2002; Pace et al., 2008). In general, all the quoted studies obtained a metallicity either barely or definitely supersolar. Of these, the high-resolution abundance determinations were derived mainly for dwarfs or early-type giants (e.g. Friel & Boesgaard, 1992; Burkhart & Coupry, 1998; An et al., 2007; Pace et al., 2008). Surprisingly, to our knowledge, there are no recent high-resolution abundance determinations of late-type giants in this cluster.

Table 11 shows a comparison of our results with some of the most recent high-resolution studies. In general, the  $[Fe/H]$  we derived in our late-type giants lies in-between those of Pace et al. (2008) and An et al. (2007), suggesting that the proposed dichotomy of literature values (barely supersolar versus definitely supersolar) should be interpreted rather as an above average uncertainty. This larger than usual uncertainty could naturally

arise from the different spectral types and abundance analysis methods employed in the literature. The  $[\text{Fe}/\text{H}]$  ratio derived by (Burkhardt & Coupry, 1998), based on Am stars, is on average  $\approx 0.3$  dex larger than the values obtained in other works using different spectral-type stars. Although these stars should in principle reflect the chemical composition of the cluster, Am stars always have overabundant Fe abundances relative to other objects in the same clusters, without a clear explanation appearing in the literature. As in the case of the Hyades, Na and O abundances derived by us appear marginally discrepant with those by Pace et al. (2008), and will be discussed in more detail in Section 5.

## 5. Discussion of abundance ratios

As in Paper I, we compared our abundance ratios (and those from Paper I) with both others in the literature and the abundances of the Galactic disc field stars from Reddy et al. (2006, 2003) in Figures 3 to 6. We extended the open cluster abundance compilation of Paper I (see Table 12) with both recent published works and old studies that were not included in the previous version. In both cases, as in Paper I, we included only studies based on high-resolution ( $R \geq 18000$ ) spectroscopy. When more than one determination was available for one cluster, we simply plotted them all to give a realistic idea of the uncertainties involved in the compilation, and we did not attempt to correct for differences between the abundance analysis procedures ( $\log g f$ , solar reference, and so on), because this would be beyond the scope of the present article.

### 5.1. Iron-peak element ratios

Figure 3 shows the abundance ratios of iron-peak elements. Our OC with abundances close to solar (i.e., Hyades, Praesepe, and NGC 752) are in very good agreement with the results obtained in other OC studied with high-resolution spectra and in disc stars of similar metallicity. A larger scatter or marginal discrepancies are sometimes observed for the odd elements Sc, V, and Co, but this is because of the well-known hyperfine structure (HFS) of the lines usually employed in the analysis. The element that appears to suffer more from these effects is vanadium. This scatter is due, at least in part, to the different procedures used in the literature for treating the HFS splitting. We stress that in our case, we do not attempt any HFS correction.

The most metal-poor and oldest OC in our sample, Be 32, has a puzzling behaviour. While all its iron-peak abundance ratios are still compatible with the literature values for OC and field stars of similar metallicity (uncertainties are large), some underlying discrepancy could be present. For example, HFS should cause an overestimate (and not an underestimate) of vanadium. In addition, chromium appears to be lower than solar. We note that (see Table 8) the literature Co and Cr determinations by Friel et al. (2010), Sestito et al. (2006), and Bragaglia et al. (2008) are very similar to ours. In the case of our  $[\text{Cr}/\text{Fe}]$  measurement for Be 32, we must note that our two giants appear to exhibit quite different  $[\text{Cr}/\text{Fe}]$  abundances, resulting in a large scatter in the cluster average value. This large scatter is most probably due to a measurement uncertainty, and should not be considered significant.

In Paper I, we noticed a peculiar behaviour in the Ni abundance ratios of literature OC determinations: they appear to be slightly richer in Ni than field stars by roughly 0.05 dex. Our  $[\text{Ni}/\text{Fe}]$  ratios are in closer agreement with the field star determinations than with the OC ones. Although this difference is small

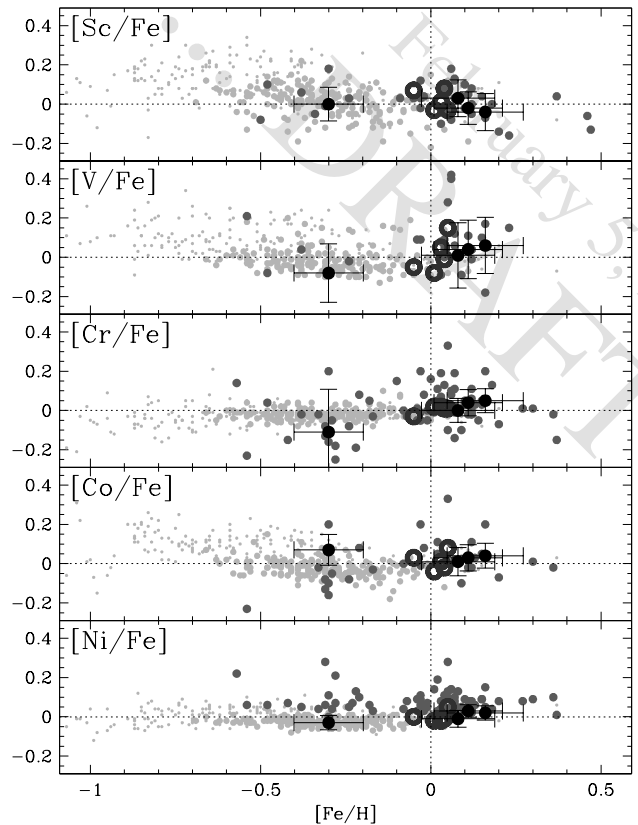


**Fig. 3.** Comparison between our iron-peak abundance ratios (large black dots), those of Paper I (large black open circles), high-resolution measurements listed in Table 12 (large dark grey dots), field stars belonging to the thin disc (light grey dots, Reddy et al., 2003), and to the thick disc (tiny light grey dots, Reddy et al., 2006). Errorbars in our measurements are the quadratic sum of all uncertainties discussed in Sections 3.2 and 3.3.

(within the uncertainties), it appears systematic in nature, and we were unable to find any easy explanation, such as the choice of either solar reference abundances or the  $\log g f$  system, of this discrepancy.

### 5.2. Alpha-element ratios

Figure 4 shows the abundance ratios of  $\alpha$ -elements. As for iron-peak elements, our measurements are always compatible with the literature values, within their uncertainties. Generally speaking, all our OC show roughly solar  $\alpha$ -enhancements, even Be 32, which has a lower metallicity.

However, some elements deserve some more discussion, as was noted in Paper I. For example, the  $\log g f$  of calcium are quite uncertain, and we chose the VALD reference atomic data, which explains why our  $[\text{Ca}/\text{Fe}]$  ratios are slightly lower than the bulk of literature determinations for cluster and disc stars. A similar problem affects the Mg lines, as can clearly be appreciated from the large spread of literature values. Our  $[\text{Mg}/\text{Fe}]$  determinations tend to lie on the upper envelope of literature ratios for OC. A deeper discussion of Mg abundances can be found in Paper I.

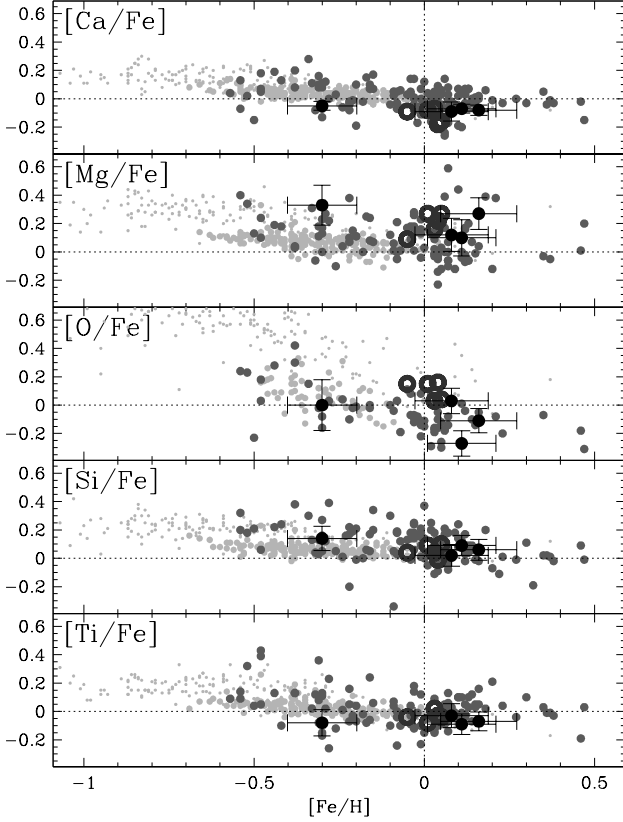


**Fig. 4.** Comparison of our  $\alpha$ -elements ratios with literature values. Symbols are the same as in Figure 3.

In the case of oxygen, the problem is instead in the difficulty in measuring its small lines. The forbidden [O I] line at 6300 Å, which we used in this paper, suffers from contamination by a Ni line and by telluric absorption features, while the O triplet around 7770 Å (used by some other studies) suffers from NLTE effects. This is reflected by the large scatter in literature values.

### 5.3. Heavy element ratios

We determined abundances for three heavy s-process elements: Ba, La, and Nd; and one light s-process element: Y (Figure 5). Literature determinations for these elements are not numerous. D’Orazi et al. (2009) measured Ba in several OC using spectral synthesis to take into account HFS. The [Ba/Fe] abundances derived by D’Orazi et al. (2009) taking into account HFS do not differ significantly from other literature determinations (including ours). The [Ba/Fe] ratios are clearly above solar for most of the clusters and they show a scatter larger than  $\sim 0.5$ . D’Orazi et al. (2009) found this scatter to be due to age: the Ba content appears to increase for younger clusters. The available lanthanum and neodymium lines were unfortunately relatively small, and we were able to find fewer published studies to compare with. As a result, the solar clusters (Hyades, Praesepe, and NGC 752) have La and Nd ratios in good agreement with the literature, while Be 32 appears to have lower [La/Fe] and [Nd/Fe] than the few studied OC at a similar metallicity, which are Mel 66 (Gratton & Contarini, 1994) and NGC 2243 (Smith & Suntzeff, 1987). However, our [Nd/Fe]

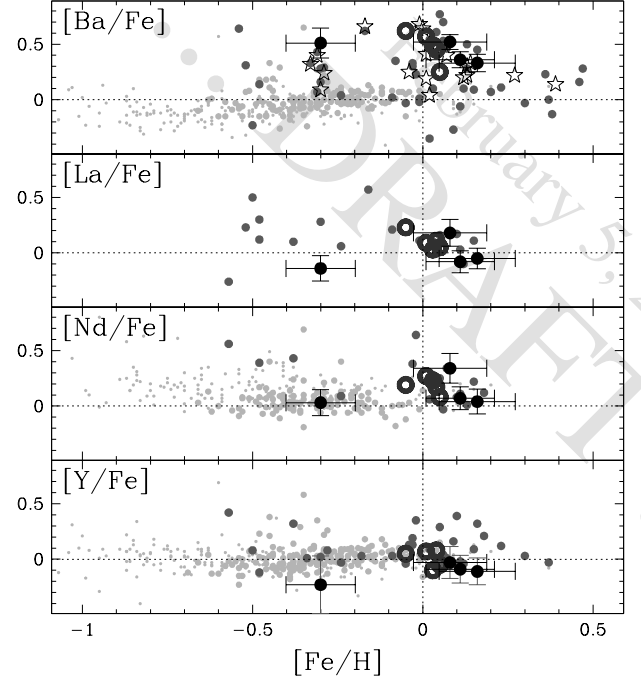


**Fig. 5.** Comparison of our s-process elements ratios with the literature ones. Symbols are the same as in Figure 3, except for the black star-like symbols in the top [Ba/Fe] panel, which represent the revision of Ba abundances with spectral synthesis performed by D’Orazi et al. (2009).

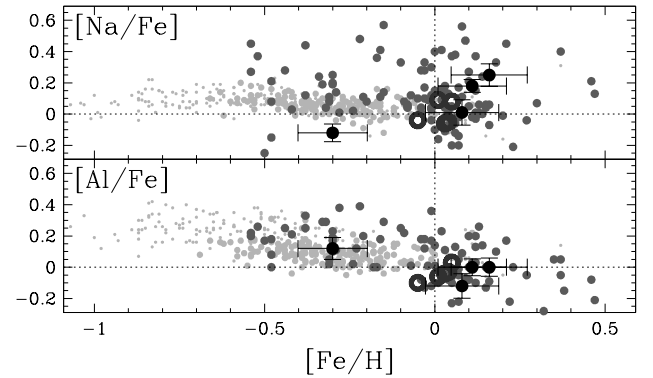


**Fig. 6.** Comparison between our [Na/Fe] and [Al/Fe] ratios and the literature ones. Symbols are the same as in Figure 3.

agrees well with the field star solar ratios. The only light s-process element we could measure, Y, relies on a couple of weak lines that provide uncertain abundances (see the large errorbar in Figure 5). Our Y ratio appears to be lower than all literature estimates, although still compatible with the solar values of field stars of similar metallicity, within the large uncertainties.

In summary, we can say that all the studied clusters appear to have roughly solar s-process enhancements, but it would be extremely interesting to attempt a more detailed study of s-process elements in OC, as done by D’Orazi et al. (2009) for barium.



#### 5.4. Ratios of Na and Al and anticorrelations

As discussed in Paper I, the study of light elements in OC is quite interesting. The elements Al and Na, together with Mg, O, C, and N, show puzzling (anti-)correlations in almost all of the studied globular clusters, in the Milky Way (see, e.g., Carretta et al., 2010; Pancino et al., 2010b, and references therein) and outside (e.g. Mucciarelli et al., 2009; Letarte et al., 2006). No (anti-)correlations were observed in either field stars (but see Martell & Grebel, 2010) or OC (Martell & Smith, 2009; de Silva et al., 2009; Smiljanic et al., 2009, and Paper I) so far. This suggests that metallicity, cluster size and age, or the environment must play a rôle, and therefore finding (anti-)correlations in some OC would be of enormous importance to put tighter constraints on the phenomenon.

We determined abundances of Al and Na and compared them with published results in Figure 6. While in the case of aluminium the agreement with literature values is good, we find a significantly lower  $[\text{Na}/\text{Fe}]$  ratio for Be 32 than for other clusters or field stars of similar metallicity. Generally speaking, the large scatter in Na determinations could be due to the difficulties in measuring Na lines, often affected by NLTE effects (Gratton et al., 1999), although no such scatter is observed among field stars. However, a few clusters have  $[\text{Na}/\text{Fe}]$  lower than our Be 32 determination, and NLTE corrections (Gratton et al., 1999) could make the discrepancy of our Be 32 Na determination even worse. Unfortunately, given the large scatter and the difficulty of measurement, it is difficult to either confirm or exclude the presence of some (small) intrinsic  $[\text{Na}/\text{Fe}]$  scatter in this clusters.

In Figure 7, all the studied stars occupy the “normal stars” loci, which is around solar for Na and Al, and slightly  $\alpha$ -enhanced for O and Mg (see Section 5.2). There is a hint of correlation between  $[\text{Al}/\text{Fe}]$  and  $[\text{Na}/\text{Fe}]$ , which was also observed for objects studied in Paper I. Of course, small variations in  $T_{\text{eff}}$  could induce artificial correlations between element pairs, so the observed trend is most probably not-significant. However, we again note that the Na spread is very large (see above), suggesting that a small degree of chemical anomalies (barely hidden within the present observational uncertainties) cannot be completely excluded.

## 6. Galactic trends

The existence of trends in the chemical abundances with Galactocentric distance,  $R_{gc}$ , vertical distance to the Galactic plane,  $z$ , and age, are key to understanding Galactic disc formation and evolution because they provide fundamental constraints on chemical evolution models. Different tracers have been used to investigate trends in the Galactic disc: OB stars (e.g. Daflon & Cunha, 2004), Cepheids (e.g. Lemasle et al., 2008), H II regions (e.g. Deharveng et al., 2000), and planetary nebulae (e.g. Costa et al., 2004). However, as coeval groups of stars at the same distance and with a homogeneous chemical composition, OC are the ideal test particles to investigate the existence of radial and vertical gradients and of an age-metallicity relation in the disc.

We complement the small sample of abundance ratios obtained here and in Paper I with a revised version of the literature data first presented in Paper I (Table 12). When a cluster had two or more abundance determinations available in the literature, we averaged them to make the figures easily readable and the error bars are, simply, calculated as the standard deviation. For those clusters with only one abundance determina-

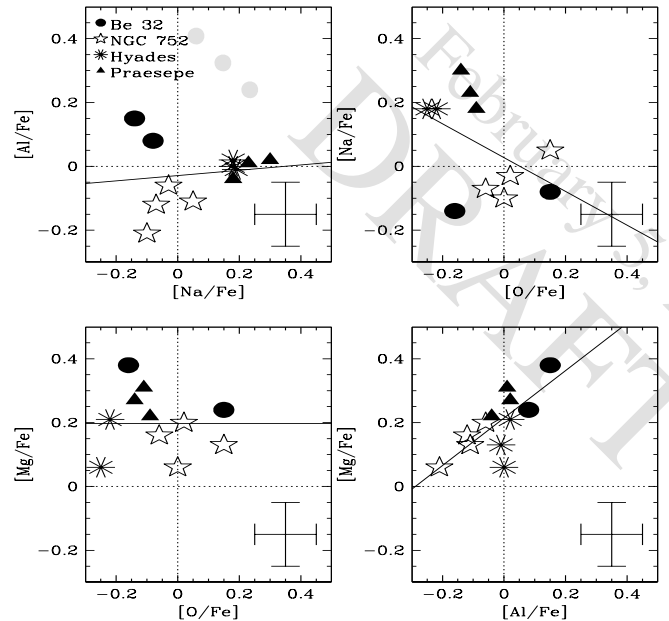


**Fig. 7.** A search for (anti-)correlations of Al, Mg, Na, and O among our target stars. The four panels show different planes of abundance ratios, where stars belonging to each cluster are marked with different symbols. Dotted lines show solar values, solid lines show linear regressions and the typical uncertainty ( $\sim 0.1$  dex) is marked at the lower right corner of each panel.

tion, the error bars are the uncertainties in those determinations. The heliocentric distances compiled in the updated version of the Dias et al. (2002) database were used to obtain  $R_{gc}$  and  $z$  for each cluster, assuming  $R_{GC\odot} = 8.5$  kpc. Ages were obtained from the same source, which is a compilation of different values available in the literature, hence might still be quite inaccurate for some clusters. In spite of its heterogeneity, our compilation contains a total of 89 clusters and is, to the best of our knowledge, the largest available in the literature, based on high-resolution spectroscopic abundances. Any attempt to homogenize this sample, for which abundances, distances, and ages have been derived from very different techniques, is clearly beyond the scope of this paper. This prevents us from a detailed analysis of the Galactic trends of all elements. For this reason, we focus only on  $[\text{Fe}/\text{H}]$  and  $[\alpha/\text{Fe}]$  ratios. In spite of this heterogeneity, this analysis is still very useful owing to the number of clusters, and the large range of ages, and vertical and radial distances covered, even if the heterogeneity of the sample forces us to be extremely cautious when drawing any conclusion from the data.

### 6.1. Trends with Galactocentric radius

Radial gradients may arise when the disc forms, and different mechanisms can produce them: for example, different timescales of star formation at different distances (e.g., Schaye, 2004); a radial variation in the infall of gas; or a change in the yield as a function of the radius (e.g., Molla et al., 1996). This initial radial gradient can be either amplified (steepened) or washed out (flattened) with time by radial mixing (e.g., Roškar et al., 2008).

Since the pioneering work of Janes (1979), OC have been widely used to investigate the gradient in metallicity with radius in the Galactic disc (e.g., Twarog et al., 2003; Friel et al.,



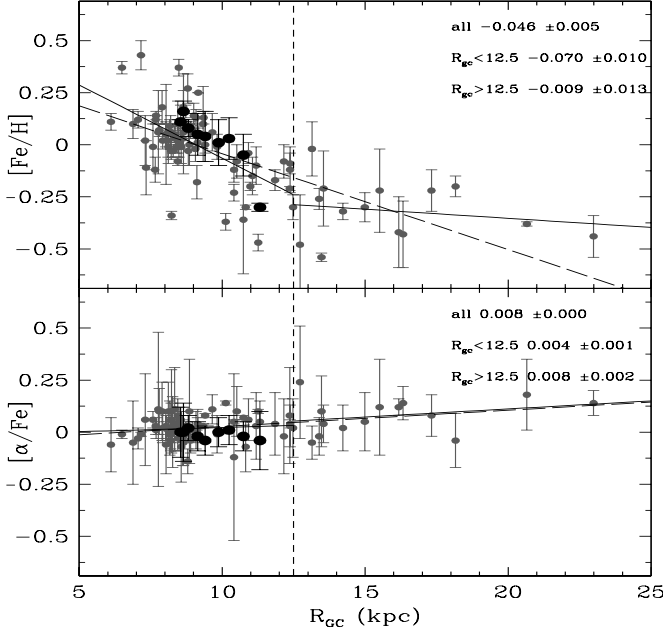


**Fig. 8.** Trends of  $[\text{Fe}/\text{H}]$  (top panel) and  $[\alpha/\text{Fe}]$  (bottom panel) with galactocentric radius. Grey dots are OC compiled in Table 12, while black dots are the ones analysed here and in Paper I. A global linear fit is drawn in both panels (long-dashed line). Two separate linear fits of OC inside and outside 12.5 kpc are also shown (solid lines).

2002; Magrini et al., 2009; Friel et al., 2010; Jacobson et al., 2011a,b). Friel (1995) reviewed the firsts investigations in this field. Since then, a great effort have been performed to obtain both homogeneous (e.g., Friel et al., 2002; Sestito et al., 2008; Friel et al., 2010) and/or larger samples (e.g., Twarog et al., 1997; Jacobson et al., 2011a,b). All these investigations agree on the fact that the iron content decreases with increasing radius (e.g., Friel et al., 2002). This behaviour has been generally considered linear with a slope between  $-0.05$  and  $-0.09 \text{ dex kpc}^{-1}$ , depending on the cluster sample used. Similar trends were obtained for other different tracers of the disc (e.g., Andrievsky et al., 2004; Lemasle et al., 2008). Most of these works were limited to the inner  $R_{gc} \approx 15 \text{ kpc}$ . However, investigations based on samples containing clusters at larger distances (e.g., Twarog et al., 1997; Yong et al., 2005; Sestito et al., 2008) found that the  $[\text{Fe}/\text{H}]$  ratio decreases as a function of increasing radius to  $R_{gc} \approx 12.5 \text{ kpc}$  and appears to flatten from there outwards.

The variation in  $[\text{Fe}/\text{H}]$  with  $R_{gc}$  in our compilation has been plotted in the top panel of Figure 8. The whole sample is well fitted by a line with a slope of  $-0.046 \pm 0.005 \text{ dex kpc}^{-1}$  (long-dashed line), in concordance with the result obtained in Paper I from a  $\approx 20\%$  smaller sample ( $-0.05 \pm 0.01 \text{ dex kpc}^{-1}$ ) and in other investigations in the literature (e.g.  $-0.06 \pm 0.02 \text{ dex kpc}^{-1}$ ; Friel et al., 2002). The sample used here contains more clusters with distances larger than  $R_{gc} \geq 12 \text{ kpc}$ . This allows us to investigate the discontinuity observed by some authors at  $R_{gc} \approx 12\text{--}13 \text{ kpc}$ . At first sight, no clear discontinuity in slope appears, partly because of the large range of  $[\text{Fe}/\text{H}]$  at this radius ( $\approx 0.5 \text{ dex}$ ) and partly as a possible consequence of the heterogeneity of our sample. However, when we fit separately clusters inwards and outwards of 12.5 kpc, we find two significantly different

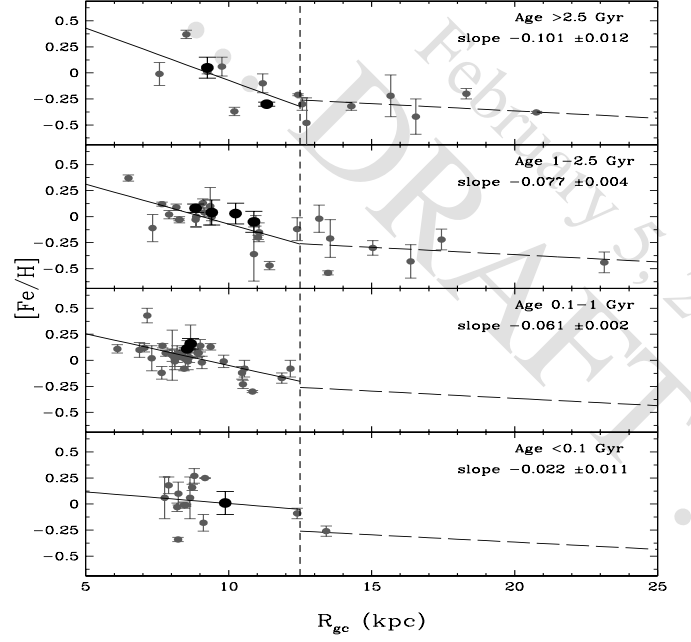


**Fig. 9.** Gradient in  $[\text{Fe}/\text{H}]$  as a function of  $R_{gc}$  in four different age bins (labeled in top-right corner). A linear fit is performed for the OC within a radius of  $R_{gc}=12.5 \text{ kpc}$ , and the slope indicated on each panel. A flatter and roughly constant slope is found outside a radius of  $R_{gc}=12.5 \text{ kpc}$ .

slopes: the metallicity in the inner disc decreases with a slope of  $-0.07 \pm 0.01 \text{ dex kpc}^{-1}$ , while in the outer disc the slope is  $-0.01 \pm 0.01 \text{ dex kpc}^{-1}$ . The obtained slopes change within the uncertainties if the cut radius varies between 11.5 and 13.5 kpc. This is also in very good agreement with the recent results by Andreuzzi et al. (2011), who find  $-0.07 \text{ dex kpc}^{-1}$  in the inner 12 kpc. This bimodal behaviour can be explained by a different chemical enrichment and star formation in the inner and outer disc; (e.g. Chiappini et al., 2001; Magrini et al., 2009) however, a sharp discontinuity between the inner and outer disc is not expected theoretically.

The ratio  $[\alpha/\text{Fe}]$  reflects the relative contributions of Type Ia and II supernovae: chemical evolution models predict an increase of this ratio with  $R_{gc}$  (e.g. Chiappini et al., 2001; Magrini et al., 2009). This tendency was indeed observed in OC by, e.g., Yong et al. (2005), Magrini et al. (2009), and in Paper I. The bottom panel of Figure 8 shows the variation in  $[\alpha/\text{Fe}]$  with  $R_{gc}$  for our compilation: a weak increase in  $\alpha$ -element abundances with radius is apparent. However, the slope is still compatible with a flat distribution at the  $1\sigma$  level, as in Paper I, especially if the two outermost clusters are removed. The discontinuity observed for  $[\text{Fe}/\text{H}]$  is not evident at all in  $[\alpha/\text{Fe}]$ .

An accretion of a satellite into the outer disc could also explain the trend observed (e.g. Chiappini et al., 2001; Yong et al., 2005). In this case, we would expect to find some inhomogeneities corresponding to the trajectory of the merger. Carraro & Bensby (2009) indeed found evidence that two OC, Berkeley 29 and Saurer 1, are related to the Sagittarius dwarf galaxy. Our compiled sample unfortunately do not allow us to investigate this question in depth.

### 6.2. Time evolution of the radial gradient

Chemical evolution models of the Galactic disc predict a variation in the metallicity gradient with time, but they disagree about the direction of this gradient variation (see Maciel et al., 2007, for a recent review), some predicting a steepening and some a flattening of the gradient with time. Studies based on metallicities derived from low-resolution spectroscopy found that old OC ( $\geq 1$  Gyr) followed a steeper radial gradient,  $\sim -0.08$  dex  $\text{kpc}^{-1}$ , than the younger ones,  $\sim -0.02$  dex  $\text{kpc}^{-1}$  (Friel et al., 2002; Chen et al., 2003). Only recently have chemical abundances been derived from high-resolution spectroscopy for a sufficient number of OC to significantly investigate the variation in the radial gradient with time. As for studies based on low-resolution spectra, they agree that the gradient was steeper in the past and has flattened with time (Magrini et al., 2009; Andreuzzi et al., 2011). For example, on the basis of a sample of  $\sim 70$  OC Andreuzzi et al. (2011) found that all objects younger than 4 Gyr display a similar gradient with a slope  $-0.07$  dex  $\text{kpc}^{-1}$  in the inner 12 kpc, while the one for older objects is steeper,  $-0.15$  dex  $\text{kpc}^{-1}$ .

Other tracers have been used to study the time variation in radial gradients. Studies based on planetary nebulae found more puzzling results: while Maciel et al. (2003) found a flattening of the gradient with time, as generally observed for OC, Stanghellini & Haywood (2010) found that the gradient steepens with time. At the moment, there is no explanation of this contradictory result. Comparisons among the slopes of the radial gradients described by populations of different ages also show that the gradient has flattened out in the past few Gyr (see Maciel & Costa, 2009, for a recent review).

To investigate the behaviour of the radial gradient in our compiled sample of high-resolution abundances, we plotted in Figure 9 the gradient in  $[\text{Fe}/\text{H}]$  as a function of  $R_{gc}$  in four different age bins. We obtained a linear fit in each age bin for the inner 12.5 kpc, and for the outer range we simply used the same fit as in Figure 8, owing to the paucity of OC after age binning in this region. We found that the slope of the  $[\text{Fe}/\text{H}]$  gradient increases as we go back in time from  $-0.02 \pm 0.01$  dex  $\text{kpc}^{-1}$  for objects younger than 0.1 Gyr to  $-0.10 \pm 0.01$  dex  $\text{kpc}^{-1}$  for clusters older than 2.5 Gyr.

### 6.3. Trends with the disc scale-height

Another interesting trend that could be investigated is the behaviour of  $[\text{Fe}/\text{H}]$  with the vertical scale-height of the disc  $z$ , i.e., the vertical  $[\text{Fe}/\text{H}]$  gradient. Although the formation of the thick discs remains an open question, the existence of vertical gradients can help us to discriminate among the mechanisms proposed to their formation. No vertical chemical gradients are expected in thick discs formed by heating caused by accretion events or major mergers. In contrast, vertical gradients may exist in discs thickened by gradual heating of the thin disc or before the gas has settled to form a thin disc (see Mould, 2005, for a review). Up to now, there is no conclusive agreement about the existence of a vertical metallicity gradient in the Galactic disc. The existence of a vertical gradient for field stars have been claimed by several authors, although they cover only about 1 kpc above and below the disc plane (Bartašiūtė et al., 2003; Marsakov & Borkova, 2005, 2006; Soubiran et al., 2008). Studies covering large ranges of  $|z|$  do not find any evidence of a vertical gradient (Gilmore et al., 1995; Soubiran & Girard, 2005; Navarro et al., 2011) among the field populations. Studies using OCs have found a vertical gra-

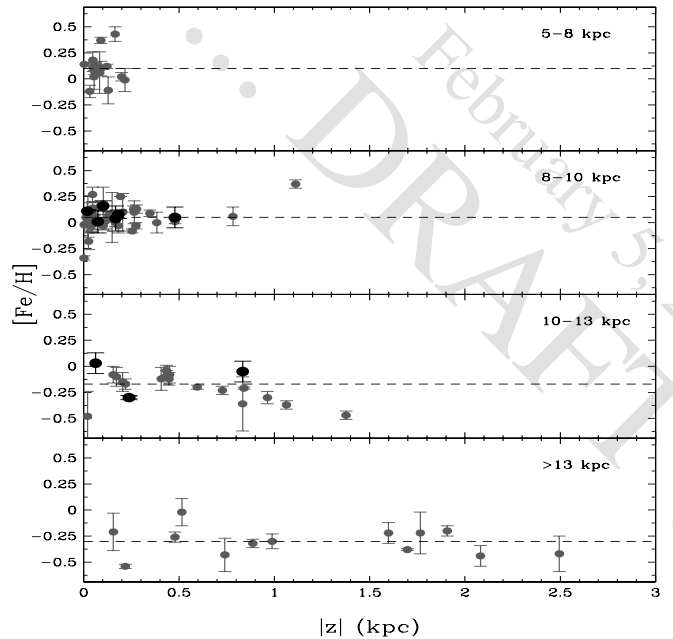


**Fig. 10.** Trends in  $[\text{Fe}/\text{H}]$  with  $|z|$  in four radial annuli as indicated on the top-right corner of each panel, moving outwards from the top to the bottom panel. Symbols are the same as in Figure 8. As a reference, we plotted dashed lines in each panel, representing the median metallicity of clusters in each radial annulus.

dient of  $\sim -0.3$  dex  $\text{kpc}^{-1}$  (Piatti et al., 1995; Carraro et al., 1998; Chen et al., 2003), although, these studies do not distinguish the effects of the radial gradient, which can mask any vertical trend. This effects were taken into account by Jacobson et al. (2011a) who found no evidence of a vertical gradient.

To investigate the presence of trends with  $z$  in our compilation, we firstly had to remove the contribution of the radial metallicity gradient. We plotted in Figure 10 the variation in  $[\text{Fe}/\text{H}]$  with  $|z|$  in four different annuli of  $R_{gc}$ . We note that OC with high  $|z|$  are preferentially located at large  $R_{gc}$ ; this is not unexpected because the disc thickens in its external regions. Moreover, an intrinsic bias caused by obscuration in the plane appears: clusters at large Galactocentric radii are found and observed preferentially higher above the plane. This could explain why the two outermost annuli studied uncover a possible weak decrease in  $[\text{Fe}/\text{H}]$  as  $z$  increases. This trend is however still compatible with no gradient at the  $1\sigma$  level and, once again, larger samples of homogeneous data are necessary to investigate this result in detail.

### 6.4. Is there an age-metallicity relation for open clusters?

Another important prediction of the chemical evolution models is the existence of an age-metallicity relation for disc populations. It is still unclear whether or not the field disc stars follow an age-metallicity relation. Some works find it (e.g. Reddy et al., 2003; Bensby et al., 2004; Reid et al., 2007), but others do not (e.g. Feltzing et al., 2001; Nordström et al., 2004; Karataş et al., 2005). Again, no clear trend of chemical abundances with age has been clearly observed in the case of Galactic OC (e.g. Friel, 1995). Although Friel et al. (2010) notices a trend of  $[\text{Al}/\text{Fe}]$  and  $[\text{O}/\text{Fe}]$  ratios with age, again larger and homogeneous samples

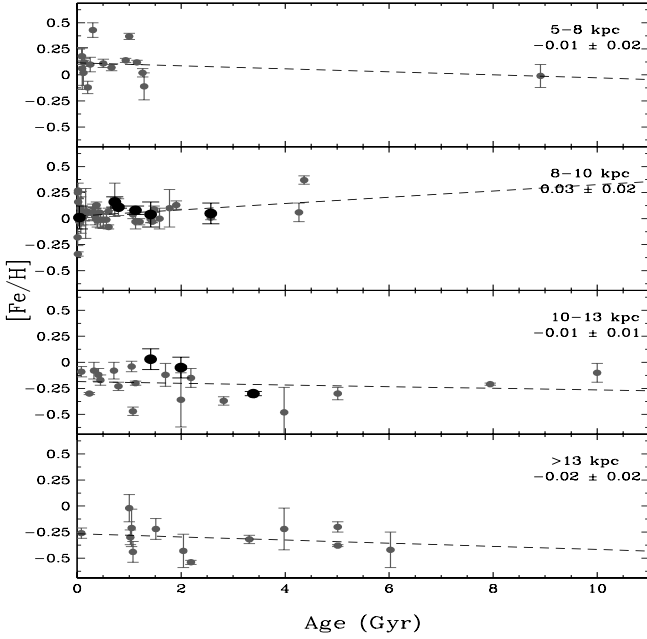


**Fig. 11.** The evolution of  $[\text{Fe}/\text{H}]$  with age in the same four radial annuli as in Figure 10. Again, dashed lines representing the median metallicity of clusters in each radial annulus have been plotted as reference.

are necessary to confirm this result. If an age-metallicity relation is confirmed for the field population but not for OC, this would imply that they might have followed a different chemical evolution (Yong et al., 2005).

The evolution of the radial gradient as a function of time, described above, indicates that the chemical enrichment of OC is modulated by their location in the Galaxy and not by the moment at which they formed. To investigate whether an age-metallicity relationship exists at a given  $R_{gc}$ , we plotted in Figure 11 the evolution of  $[\text{Fe}/\text{H}]$  with age in four different radial annuli. There is no clear trend in any of the studied annuli, although not all of them contain clusters covering the same age range. Only in the outermost annulus is a weak trend observed, although it is still not very significant. Again, we conclude that a larger sample of homogeneous data are necessary to investigate this point in depth.

## 7. Summary and conclusions

We have enlarged our sample of homogeneous high-resolution abundance measurements from the five clusters of Paper I to a total of nine, analysing here spectra of red clump giants in the Hyades, Praesepe, NGC 752, and Be 32. Our main results can be summarized as follows:

- We provide the first high-resolution based abundance ratios (other than  $[\text{Fe}/\text{H}]$ , see Sestito et al., 2008) for NGC 752, which turned out to be mostly of solar composition;
- We have presented the abundance ratios of Praesepe red clump giants, which appear to solve a puzzling dichotomy of literature determinations for stars of different evolutionary stages;
- We have found that our abundance ratios for the Hyades and Berkeley 32 are in good agreement with other literature determinations;

- We have confirmed the absence of light elements (anti-)correlations in the OC studied so far.

We have updated our compilation of previous literature data for 57 clusters of Paper I to a total of 89 clusters presented here. With this updated compilation and our homogeneous measurements in hand, we have investigated Galactic trends in  $[\text{Fe}/\text{H}]$  (and  $[\alpha/\text{Fe}]$ ) with age, Galactocentric radius, and height above the Galactic plane. Our findings are in substantial agreement with other similar investigations, where the abundance gradient appears to indeed flatten out outside  $R_{gc} \approx 12.5$  kpc, and the inner disc slope appears to flatten for younger ages as well, although the age bins are not too well-sampled. At the same time,  $[\alpha/\text{Fe}]$  shows a weak increase with  $R_{gc}$ . No significant gradients are observed with  $|z|$  or age, except for a weak tendency of  $[\text{Fe}/\text{H}]$  to decrease with increasing  $|z|$  and decrease with age in the outermost disc annulus studied. None of our measured weak trends have any significance above  $1\sigma$ . Larger samples of homogeneous data are still necessary to investigate the existence of any dependence on age and  $|z|$  in the Galactic disc.

**Acknowledgements.** We acknowledge the anonymous referee for helping us to improve this paper. R. C acknowledges the support from the Spanish Ministry of Science and Technology (Plan Nacional de Investigación Científica, Desarrollo, e Investigación Tecnológica, AYA2004-06343 and AYA2007-3E3507). R. C. also acknowledges the funds by the Spanish Ministry of Science and Innovation under the Juan de la Cierva and MEC/Fullbright fellowships, and by the Centro de Investigaciones de Astronomía (Venezuela) under its postdoctoral fellowship programme.

## References

- Alonso, A., Arribas, S., & Martínez-Roger, C. 1999, *A&AS*, 140, 261  
 An, D., Terndrup, D. M., Pinsonneault, M. H., Paulson, D. B., Hanson, R. B., & Stauffer, J. R. 2007, *ApJ*, 655, 233  
 Andersen, J. 1999, *Transactions of the IAU*, Vol. XXIVA, p.36 (1999), 24, A36  
 Andreuzzi, G., Bragaglia, A., Tosi, M., & Marconi, G. 2011, *MNRAS*, 412, 1265  
 Andrievsky, S. M., Luck, R. E., Martin, P., & Lépine, J. R. D. 2004, *A&A*, 413, 159  
 Arp, H. 1962, *ApJ*, 136, 66  
 Barry, D. C., Cromwell, R. H., & Hege, E. K. 1987, *ApJ*, 315, 264  
 Bartašiūtė, S., Aslan, Z., Boyle, R. P., Kharchenko, N. V., Ossipkov, L. P., & Sperauskas, J. 2003, *Baltic Astronomy*, 12, 539  
 Bartašiūtė, S., Deveikis, V., Straizys, V., & Bogdanovičius, A. 2007, *Baltic Astronomy*, 16, 199  
 Bensby, T., Feltzing, S., & Lundström, I. 2004, *A&A*, 421, 969  
 Bessell, M. S. 1979, *PASP*, 91, 589  
 Blake, R. M. 2002, *Ph.D. Thesis*,  
 Blake, R. M., & Rucinski, S. M. 2004, *Bulletin of the American Astronomical Society*, 36, 1483  
 Boesgaard, A. M. 1989, *ApJ*, 336, 798  
 Boesgaard, A. M., & Friel, E. D. 1990, *ApJ*, 35  
 Boesgaard, A. M. 1991, *ApJ*, 370, L95  
 Boesgaard, A. M., Jensen, E. E. C., & Deliyannis, C. P. 2009, *AJ*, 137, 4949  
 Bouvier, J., et al. 2008, *A&A*, 481, 661  
 Boyarchuk, A. A., Antipova, L. I., Boyarchuk, M. E., & Savanov, I. S. 2000, *Astronomy Reports*, 44, 76  
 Bragaglia, A., et al. 2001, *AJ*, 121, 327  
 Bragaglia, A., Sestito, P., Villanova, S., Carretta, E., Randich, S., & Tosi, M. 2008, *A&A*, 480, 79  
 Brown, J. A., Wallerstein, G., Geisler, D., & Oke, J. B. 1996, *AJ*, 112, 1551  
 Burkhart, C., & Coupry, M. F. 1998, *A&A*, 338, 1073  
 Burkhart, C., & Coupry, M. F. 2000, *A&A*, 354, 216  
 Cardelli, J. A., Clayton, G. C., & Mathis, J. S. 1989, *ApJ*, 345, 245  
 Carraro, G., Bertelli, G., Bressan, A., & Chiosi, C. 1993, *A&AS*, 101, 381  
 Carraro, G., & Chiosi, C. 1994, *A&A*, 287, 761  
 Carraro, G., Ng, Y. K., & Portinari, L. 1998, *MNRAS*, 296, 1045  
 Carraro, G., Bresolin, F., Villanova, S., Matteucci, F., Patat, F., & Romaniello, M. 2004, *AJ*, 128, 1676  
 Carraro, G., Villanova, S., Demarque, P., McSwain, M. V., Piotto, G., & Bedin, L. R. 2006, *ApJ*, 643, 1151  
 Carraro, G., de La Fuente Marcos, R., Villanova, S., Moni Bidin, C., de La Fuente Marcos, C., Baumgardt, H., & Solivella, G. 2007a, *A&A*, 466, 931



- Carraro, G., Geisler, D., Villanova, S., Frinchaboy, P. M., & Majewski, S. R. 2007b, *A&A*, 476, 217
- Carraro, G., Villanova, S., Demarque, P., Moni Bidin, C., & McSwain, M. V. 2008, *MNRAS*, 386, 1625
- Carraro, G., & Bensby, T. 2009, *MNRAS*, 397, L106
- Carretta, E., Bragaglia, A., Gratton, R. G., & Tosi, M. 2004, *A&A*, 422, 951
- Carretta, E., Bragaglia, A., Gratton, R. G., & Tosi, M. 2005, *A&A*, 441, 131
- Carretta, E., Bragaglia, A., & Gratton, R. G. 2007, *A&A*, 473, 129
- Carretta, E., Bragaglia, A., Gratton, R. G., Recio-Blanco, A., Lucatello, S., D'Orazi, V., & Cassisi, S. 2010, *A&A*, 516, A55
- Cayrel, R., et al. 2004, *A&A*, 416, 1117
- Chen, L., Hou, J. L. & Wang, J. J. 2003, *AJ*, 125, 1397
- Chiappini, C., Matteucci, F., & Romano, D. 2001, *ApJ*, 554, 1044
- Claria, J. J., Piatti, A. E., & Osborn, W. 1996, *PASP*, 108, 672
- Coleman, L. A. 1982, *AJ*, 87, 369
- Costa, R. D. D., Uchida, M. M. M., & Maciel, W. J. 2004, *A&A*, 423, 199
- Crawford, D. L., & Barnes, J. V. 1970, *AJ*, 75, 946
- Cutri, R. M., Skrutskie, M. F., Van Dyk, et al. 2003, Explanatory Supplement to the 2MASS All Sky Data Release
- Daflon, S., & Cunha, K. 2004, *ApJ*, 617, 1115
- Daniel, S. A., Latham, D. W., Mathieu, R. D., & Twarog, B. A. 1994, *PASP*, 106, 281
- Dean, J. F., Warren, P. R., & Cousins, A. W. J. 1978, *MNRAS*, 183, 569
- Deharveng, L., Peña, M., Caplan, J., & Costero, R. 2000, *MNRAS*, 311, 329
- Den Hartog, E. A., Lawler, J. E., Sneden, C., Cowan, J. J. 2003, *ApJS*, 148, 543
- De Silva, G. M., Sneden, C., Paulson, D. B., Asplund, M., Bland-Hawthorn, J., Bessell, M. S., & Freeman, K. C. 2006, *AJ*, 131, 455
- De Silva, G. M., Freeman, K. C., Asplund, M., Bland-Hawthorn, J., Bessell, M. S., & Collet, R. 2007, *AJ*, 133, 1161
- de Silva, G. M., Gibson, B. K., Lattanzio, J., & Asplund, M. 2009, *A&A*, 500, L25
- Dias, W. S., Alessi, B. S., Moitinho, A., & Lépine, J. R. D. 2002, *A&A*, 389, 871
- Dinescu, D. I., Demarque, P., Guenther, D. B., & Pinsonneault, M. H. 1995, *AJ*, 109, 2090
- D'Orazi, V., Bragaglia, A., Tosi, M., Di Fabrizio, L., & Held, E. V. 2006, *MNRAS*, 368, 471
- D'Orazi, V., Magrini, L., Randich, S., Galli, D., Busso, M., & Sestito, P. 2009, *ApJ*, 693, L31
- D'Orazi, V., & Randich, S. 2009, *A&A*, 501, 553
- Dutra, C. M., & Bica, E. 2000, *A&A*, 359, 347
- Dzervitis, U., & Paupers, O. 1993, *Ap&SS*, 199, 77
- Edvardsson, B., Andersen, J., Gustafsson, B., Lambert, D. L., Nissen, P. E., Tomkin, J., 1993, *A&A*, 275, 101
- Edvardsson, B., Pettersson, B., Kharrazi, M., & Westerlund, B. 1995, *A&A*, 293, 75
- Eggen, O. J. 1963, *ApJ*, 138, 356
- Eggen, O. J. 1989, *PASP*, 101, 54
- Eggen, O. J. 1998, *AJ*, 116, 284
- Famaey, B., Jorissen, A., Luri, X., Mayor, M., Udry, S., Dejonghe, H., & Turon, C. 2005, *A&A*, 430, 165
- Famaey, B., Pont, F., Luri, X., Udry, S., Mayor, M., & Jorissen, A. 2007, *A&A*, 461, 957
- Feltzing, S., Holmberg, J., & Hurley, J. R. 2001, *A&A*, 377, 911
- Ford, A., Jeffries, R. D., & Smalley, B. 2005, *MNRAS*, 364, 272
- Fossati, L., Folsom, C. P., Bagnulo, S., Grunhut, J. H., Kochukhov, O., Landstreet, J. D., Paladini, C., & Wade, G. A. 2011, *MNRAS*, 413, 1132
- Francic, S. P. 1989, *AJ*, 98, 888
- Friel, E. D., & Boesgaard, A. M. 1992, *ApJ*, 387, 170
- Friel E.D., Janes K.A. 1993 *A&A*, 267, 75
- Friel, E. D. 1995, *ARA&A*, 33, 381
- Friel, E. D., Janes, K. A., Tavaréz, M., Scott, J., Katsanis, R., Lotz, J., Hong, L., & Miller, N. 2002, *AJ*, 124, 2693
- Friel, E. D., Jacobson, H. R., Barrett, E., Fullton, L., Balachandran, S. C., & Pilachowski, C. A. 2003, *AJ*, 126, 2372
- Friel, E. D., Jacobson, H. R., & Pilachowski, C. A. 2005, *AJ*, 129, 2725
- Friel, E. D., Jacobson, H. R., & Pilachowski, C. A. 2010, *AJ*, 139, 1942
- Frinchaboy, P. M., Marino, A. F., Villanova, S., Carraro, G., Majewski, S. R., & Geisler, D. 2008, *MNRAS*, 391, 39
- Fulbright, J. P., McWilliam, A., & Rich, R. M. 2007, *ApJ*, 661, 1152
- Gáspár, A., Rieke, G. H., Su, K. Y. L., Balog, Z., Trilling, D., Muzzerole, J., Apai, D., & Kelly, B. C. 2009, *ApJ*, 697, 1578
- Gebran, M., Monier, R., & Richard, O. 2008, *A&A*, 479, 189
- Gebran, M., & Monier, R. 2008, *A&A*, 483, 567
- Giardino, G., Pillitteri, I., Favata, F., & Micela, G. 2008, *A&A*, 490, 113
- Gilmore, G., Wyse, R. F. G., & Jones, J. B. 1995, *AJ*, 109, 1095
- Girardi, L., Mermilliod, J.-C., & Carraro, G. 2000, *A&A*, 354, 892
- Girardi, L., & Salaris, M. 2001, *MNRAS*, 323, 109
- Gonzalez, G., & Lambert, D. L. 1996, *AJ*, 111, 424
- Gonzalez, G., & Wallerstein, G. 2000, *PASP*, 112, 1081
- Gratton, R. G., & Contarini, G. 1994, *A&A*, 283, 911
- Gratton, R. G., Carretta, E., Eriksson, K., Gustafsson, B. 1999, *A&A*, 350, 955
- Grevesse, N., Noels, A., & Sauval, A. J. 1996, *ASP Conf. Ser.* 99: Cosmic Abundances, 99, 117
- Griffin, R. F., Griffin, R. E. M., Gunn, J. E., & Zimmerman, B. A. 1988, *AJ*, 96, 172
- Hamdani, S., North, P., Mowlavi, N., Raboud, D., & Mermilliod, J.-C. 2000, *A&A*, 360, 509
- Hardy, E. 1979, *AJ*, 84, 319
- Heinemann, K. 1926, *Astronomische Nachrichten*, 227, 193
- Hernandez, M. M., Perez Hernandez, F., Michel, E., Belmonte, J. A., Goupil, M. J., & Lebreton, Y. 1998, *A&A*, 338, 511
- Hertzsprung, E. 1909, *ApJ*, 30, 135
- Hill, V., & Pasquini, L. 1999, *A&A*, 348, L21
- Hobbs, L. M., & Thorburn, J. A. 1992, *AJ*, 104, 669
- Høg, E., et al. 2000, *A&A*, 355, L27
- Hui-Bon-Hoa, A., & Alecian, G. 1998, *A&A*, 332, 224
- Jacobson, H. R., Friel, E. D., & Pilachowski, C. A. 2007, *AJ*, 134, 1216
- Jacobson, H. R., Friel, E. D., & Pilachowski, C. A. 2008, *AJ*, 135, 2341
- Jacobson, H. R., Friel, E. D., & Pilachowski, C. A. 2009, *AJ*, 137, 4753
- Jacobson, H. R., Friel, E. D., & Pilachowski, C. A. 2011a, *AJ*, 141, 58
- Jacobson, H. R., Pilachowski, C. A., & Friel, E. D. 2011b, *AJ*, 142, 59
- Jacquinet-Husson, N., Ari, E., Ballard, J., Barbe, A., Bjoraker, G. et al. 1999, *JQSRT*, 62, 205
- Jacquinet-Husson, N., Scott, N. A., Garceran, K., Armante, R., Chédin, A. 2005, *JQSRT*, 95, 429
- Jameson, R. F., Lodieu, N., Casewell, S. L., Bannister, N. P., & Dobbie, P. D. 2008, *MNRAS*, 385, 1771
- Janes, K. A. 1979, *ApJS*, 39, 135
- Jennens, P. A., & Helfer, H. L. 1975, *MNRAS*, 172, 681
- Johansson, S., Litzén, U., Lundberg, H., & Zhang, Z. 2003, *ApJ*, 584, L107
- Johnson, H. L. 1952, *ApJ*, 116, 640
- Johnson, H. L. 1953, *ApJ*, 117, 356
- Johnson, H. L., & Knuckles, C. F. 1955, *ApJ*, 122, 209
- Johnson, H. L. 1961, *Lowell Observatory Bulletin*, 5, 133
- Johnson, H. L., Iriarte, B., Mitchell, R. I., & Wisniewski, W. Z. 1966, *Communications of the Lunar and Planetary Laboratory*, 4, 99
- Kaluzny, J., & Mazur, B. 1991, *Acta Astronomica*, 41, 167
- Karataş, Y., Bilir, S., & Schuster, W. J. 2005, *MNRAS*, 360, 1345
- King, J. R., Soderblom, D. R., Fischer, D., & Jones, B. F. 2000, *ApJ*, 533, 944
- Klein Wassink, W. J. 1927, *Publications of the Kapteyn Astronomical Laboratory Groningen*, 41, 1
- Komarov, N. S., & Basak, N. Y. 1993, *AZh*, 70, 111
- Kraus, A. L., & Hillenbrand, L. A. 2007, *AJ*, 134, 2340
- Kupka, F., Piskunov, N., Ryabchikova, T. A., Stempels, H. C., & Weiss, W. W. 1999, *A&AS*, 138, 119
- Lata, S., Pandey, A. K., Sagar, R., & Mohan, V. 2002, *A&A*, 388, 158
- Lemasle, B., François, P., Piersimoni, A., Pedicelli, S., Bono, G., Laney, C. D., Primas, F., & Romaniello, M. 2008, *A&A*, 490, 613
- Letarte, B., Hill, V., Jablonka, P., Tolstoy, E., François, P., & Meylan, G. 2006, *A&A*, 453, 547
- Loktin, A. V. 2000, *Astronomy Letters*, 26, 657
- Loktin, A. V., & Beshenov, G. V. 2001, *Astronomy Letters*, 27, 386
- Luck, R. E. 1994, *ApJS*, 91, 309
- Luck, R. E., & Challener, S. L. 1995, *AJ*, 110, 2968
- Maciel, W. J., Costa, R. D. D., & Uchida, M. M. M. 2003, *A&A*, 397, 667
- Maciel, W. J., Quireza, C., & Costa, R. D. D. 2007, *A&A*, 463, L13
- Maciel, W. J., & Costa, R. D. D. 2009, *IAU Symposium*, 254, 38P
- Maeder, A. 1971, *A&A*, 10, 354
- Magain, P. 1984, *A&A*, 134, 189
- Magrini, L., Sestito, P., Randich, S., & Galli, D. 2009, *A&A*, 494, 95
- Magrini, L., Randich, S., Zoccali, M., Jilkova, L., Carraro, G., Galli, D., Maiorca, E., & Busso, M. 2010, *A&A*, 523, 11
- Mallik, S. V. 1998, *A&A*, 338, 623
- Marsakov, V. A., & Borkova, T. V. 2005, *Astronomy Letters*, 31, 515
- Marsakov, V. A., & Borkova, T. V. 2006, *Astronomy Letters*, 32, 376
- Martell, S. L., & Smith, G. H. 2009, *PASP*, 121, 577
- Martell, S. L., & Grebel, E. K. 2010, *A&A*, 519, A14
- Mathieu, R. D., & Mazeh, T. 1988, *ApJ*, 326, 256
- Mazzei, P., & Pigatto, L. 1988, *A&A*, 193, 148
- Mendoza, E. E. 1967, *Boletín de los Observatorios Tonantzintla y Tacubaya*, 4, 149
- Mermilliod, J.-C. 1995, *ASSL Vol. 203: Information & On-Line Data in Astronomy*, 127
- Mermilliod, J.-C., Mathieu, R. D., Latham, D. W., & Mayor, M. 1998, *A&A*, 339, 423



- Mermilliod, J.-C., Andersen, J., Latham, D. W., & Mayor, M. 2007, *A&A*, 473, 829
- Meynet, G., Mermilliod, J.-C., & Maeder, A. 1993, *A&AS*, 98, 477
- Mikolaitis, Š., Tautvaišienė, G., Gratton, R., Bragaglia, A., & Carretta, E. 2010, *MNRAS*, 407, 1866
- Mikolaitis, Š., Tautvaišienė, G., Gratton, R., Bragaglia, A., & Carretta, E. 2011a, *MNRAS*, 413, 2199
- Mikolaitis, Š., Tautvaišienė, G., Gratton, R., Bragaglia, A., & Carretta, E. 2011b, arXiv:1105.4047
- Milone, E. F., Stagg, C. R., Sugars, B. A., McVean, J. R., Schiller, S. J., Kallrath, J., & Bradstreet, D. H. 1995, *AJ*, 109, 359
- Mishenina, T. V., Bienaymé, O., Gorbaneva, T. I., Charbonnel, C., Soubiran, C., Korotin, S. A., & Kovtyukh, V. V. 2006, *A&A*, 456, 1109
- Mishenina, T. V., Gorbaneva, T. I., Bienaymé, O., Soubiran, C., Kovtyukh, V. V., & Orlova, L. F. 2007, *Astronomy Reports*, 51, 382
- Molla, M., Ferrini, F., & Diaz, A. I. 1996, *ApJ*, 466, 668
- Montegriffo, P., Ferraro, F. R., Origlia, L., & Fusi Pecci, F. 1998, *MNRAS*, 297, 872
- Monroe, T. R., & Pilachowski, C. A. 2010, *AJ*, 140, 2109
- Mould, J. 2005, *AJ*, 129, 698
- Mucciarelli, A., Origlia, L., Ferraro, F. R., & Pancino, E. 2009, *ApJ*, 695, L134
- Mucciarelli, A. 2011, *A&A*, 528, 44
- Narayanan, V. K., & Gould, A. 1999, *ApJ*, 515, 256
- Navarro, J. F., Abadi, M. G., Venn, K. A., Freeman, K. C., & Anguiano, B. 2011, *MNRAS*, 412, 1203
- Nicolet, B. 1981, *A&A*, 104, 185
- Nissen, P. E. 1988, *A&A*, 199, 146
- Nordström, B., et al. 2004, *A&A*, 418, 989
- Origlia, L., Valenti, E., Rich, R. M., & Ferraro, F. R. 2006, *ApJ*, 646, 499
- Pace, G., Pasquini, L., & François, P. 2008, *A&A*, 489, 403
- Pace, G., Danziger, J., Carraro, G., Melendez, J., François, P., Matteucci, F., & Santos, N. C. 2010, *A&A*, 515, A28
- Pancino, E., Carrera, R., Rossetti, E., & Gallart, C. 2010, *A&A*, 511, 56. Paper I
- Pancino, E., Rejkuba, M., Zoccali, M., & Carrera, R. 2010, *A&A*, 524, A44
- Pasquini, L., Randich, S., Zoccali, M., Hill, V., Charbonnel, C., & Nordström, B. 2004, *A&A*, 424, 951
- Patenaude, M. 1978, *A&A*, 66, 225
- Paulson, D. B., Sneden, C., & Cochran, W. D. 2003, *AJ*, 125, 3185
- Pereira, C. B., & Quireza, C. 2010, *IAU Symposium*, 266, 495
- Percival, S. M., Salaris, M., & Kilkeny, D. 2003, *A&A*, 400, 541
- Perryman, M. A. C., et al. 1997, *A&A*, 323, L49
- Perryman, M. A. C., et al. 1998, *A&A*, 331, 81
- Peterson, R. C., & Green, E. M. 1998, *ApJ*, 502, L39
- Pfeiffer, M. J., Frank, C., Baumüller, D., Fuhrmann, K., & Gehren, T. 1998, *A&AS*, 130, 381
- Piatti, A. E., Claria, J. J., & Abadi, M. G. 1995, *AJ*, 110, 2813
- Pinsonneault, M. H., Stauffer, J., Soderblom, D. R., King, J. R., & Hanson, R. B. 1998, *ApJ*, 504, 170
- Platais, I., Melo, C., Fulbright, J. P., Kozhurina-Platais, V., Figueira, P., Barnes, S. A., & Méndez, R. A. 2008, *MNRAS*, 391, 1482
- Pourbaix, D., et al. 2004, *A&A*, 424, 727
- Ramírez, S. V., & Cohen, J. G. 2003, *AJ*, 125, 224
- Randich, S., Pallavicini, R., Meola, G., Stauffer, J. R., & Balachandran, S. C. 2001, *A&A*, 372, 862
- Randich, S., Sestito, P., & Pallavicini, R. 2003, *A&A*, 399, 133
- Randich, S., Sestito, P., Primas, F., Pallavicini, R., & Pasquini, L. 2006, *A&A*, 450, 557
- Reddy, B. E., Tomkin, J., Lambert, D. L., & Allende Prieto, C. 2003, *MNRAS*, 340, 304
- Reddy, B. E., Lambert, D. L., & Allende Prieto, C. 2006, *MNRAS*, 367, 1329
- Reid, I. N., Turner, E. L., Turnbull, M. C., Mountain, M., & Valenti, J. A. 2007, *ApJ*, 665, 767
- Richtler, T., & Sagar, R. 2001, *Bulletin of the Astronomical Society of India*, 29, 53
- Roman, N. G. 1955, *ApJ*, 121, 454
- Rohlf, K., & Vanysek, V. 1962, *Astronomische Abhandlungen der Hamburger Sternwarte*, 5, 341
- Roškar, R., Debattista, V. P., Quinn, T. R., Stinson, G. S., & Wadsley, J. 2008, *ApJ*, 684, L79
- Salaris, M., Weiss, A., & Percival, S. M. 2004, *A&A*, 414, 163
- Santos, N. C., Lovis, C., Pace, G., Melendez, J., & Naef, D. 2009, *A&A*, 493, 309
- Schuler, S. C., King, J. R., Fischer, D. A., Soderblom, D. R., & Jones, B. F. 2003, *AJ*, 125, 2085
- Schuler, S. C., Hatzes, A. P., King, J. R., Kürster, M., & The, L.-S. 2006, *AJ*, 131, 1057
- Schuler, S. C., King, J. R., & The, L.-S. 2009, *ApJ*, 701, 837
- Sestito, P., Randich, S., Mermilliod, J.-C., & Pallavicini, R. 2003, *A&A*, 407, 289
- Sestito, P., Randich, S., & Pallavicini, R. 2004, *A&A*, 426, 809
- Sestito, P., Bragaglia, A., Randich, S., Carretta, E., Prisinzano, L., & Tosi, M. 2006, *A&A*, 458, 121
- Sestito, P., Randich, S., & Bragaglia, A. 2007, *A&A*, 465, 185
- Sestito, P., Bragaglia, A., Randich, S., Pallavicini, R., Andrievsky, S. M., & Korotin, S. A. 2008, *A&A*, 488, 943
- Schaye, J. 2004, *ApJ*, 609, 667
- Shen, Z.-X., Jones, B., Lin, D. N. C., Liu, X.-W., & Li, S.-L. 2005, *ApJ*, 635, 608
- Skrutskie, M. F., et al. 2006, *AJ*, 131, 1163
- Smiljanic, R., Gauderon, R., North, P., Barbuy, B., Charbonnel, C., & Mowlavi, N. 2009, *A&A*, 502, 267
- Smith, V. V., & Suntzeff, N. B. 1987, *AJ*, 93, 359
- Soderblom, D. R., Laskar, T., Valenti, J. A., Stauffer, J. R., & Rebull, L. M. 2009, *AJ*, 138, 1292
- Soubiran, C., & Girard, P. 2005, *A&A*, 438, 139
- Soubiran, C., Bienaymé, O., Mishenina, T. V., & Kovtyukh, V. V. 2008, *A&A*, 480, 91
- Spite, M. 1967, *Annales d'Astrophysique*, 30, 211
- Stanghellini, L., & Haywood, M. 2010, *ApJ*, 714, 1096
- Stetson, P. B., & Pancino, E. 2008, *PASP*, 120, 1332
- Tadross, A. L. 2001, *New Astronomy*, 6, 293
- Tautvaišienė, G., Edvardsson, B., Tuominen, I., Ilyin, I. 2000, *A&A*, 360, 499
- Tautvaišienė, G., Edvardsson, B., Puzeras, E., & Ilyin, I. 2005, *A&A*, 431, 933
- Taylor, B. J. 2006, *AJ*, 132, 2453
- Taylor, B. J. 2007, *AJ*, 134, 934
- Terndrup, D. M., Pinsonneault, M., Jeffries, R. D., Ford, A., Stauffer, J. R., & Sills, A. 2002, *ApJ*, 576, 950
- Tosi, M., Bragaglia, A., & Cignoni, M. 2007, *MNRAS*, 378, 730
- Tsvetkov, T. G. 1993, *Ap&SS*, 203, 247
- Twarog, B. A. 1983, *ApJ*, 267, 207
- Twarog, B. A., Ashman, K. M., & Anthony-Twarog, B. J. 1997, *AJ*, 114, 2556
- Twarog, B. A., Anthony-Twarog, B. J., & De Lee, N. 2003, *AJ*, 125, 1383
- van Bueren, H. G. 1952, *Bull. Astron. Inst. Netherlands*, 11, 385
- van den Heuvel, E. P. J. 1969, *PASP*, 81, 815
- van Leeuwen, F. 1999, *A&A*, 341, L71
- Varenne, O., & Monier, R. 1999, *A&A*, 351, 247
- Villanova, S., Carraro, G., Bresolin, F., & Patat, F. 2005, *AJ*, 130, 652
- Villanova, S., Baume, G., & Carraro, G. 2007, *MNRAS*, 379, 1089
- Villanova, S., Carraro, G., & Saviane, I. 2009, *A&A*, 504, 845
- Villanova, S., Geisler, D., & Piotto, G. 2010, *ApJ*, 722, L18
- Yong D., Carney B.W., & Teixeira de Almeida M.L. 2005, *AJ*, 130, 597

**Table 12.** Literature sources of high-resolution ( $R \geq 1500$ ) [Fe/H] ratios of open clusters together with the resolution, signal-to-noise ratios, number of stars, and method used in each of them.

Cluster	[Fe/H]	Resolution	S/N	N. Star	Method	References
Be 17	$-0.10 \pm 0.09$	25000	$\geq 80$	3 giant	EW <sup>1</sup>	Friel et al. (2005)
Be 20	$-0.48 \pm 0.08$	28000	$\geq 50$	2 giant	EW	Yong et al. (2005)
	$-0.30 \pm 0.02$	45000	$\geq 35$	2 giant	EW	Sestito et al. (2008)
Be 21	$-0.54 \pm 0.02$	48000	$\sim 20$	4 giants	EW	Hill & Pasquini (1999)
Be 22	$-0.32 \pm 0.04$	34000	20–25	2 K giant	EW	Villanova et al. (2005)
Be 25	$-0.20 \pm 0.05$	40000	25–40	4 giant	EW	Carraro et al. (2007b)
Be 29	$-0.44 \pm 0.02$	34000	$\sim 70$	2 G giant	EW	Carraro et al. (2004)
	$-0.52 \pm 0.03$	28000	$\geq 100$	2 giant	EW	Yong et al. (2005)
	$-0.31 \pm 0.03$	45000	$\geq 25$	6 giant	EW	Sestito et al. (2008)
Be 31	$-0.54 \pm 0.06$	28000	$\geq 60$	1 giant	EW	Yong et al. (2005)
	$-0.31 \pm 0.06$	28000	$\sim 100$	2 giant	EW <sup>1</sup>	Friel et al. (2010)
Be 32	$-0.29 \pm 0.04$	45000	$\geq 50$	9 giant	EW	Bragaglia et al. (2008)
	$-0.30 \pm 0.02$	28000	$\sim 100$	2 giant	EW <sup>1</sup>	Friel et al. (2010)
Be 39	$-0.21 \pm 0.01$	28000	70–115	3 giant	EW <sup>1</sup>	Friel et al. (2010)
Be 66	$-0.48 \pm 0.24$	34000	5–15	2 K giant	EW	Villanova et al. (2005)
Be 73	$-0.22 \pm 0.10$	40000	25–40	2 giant	EW	Carraro et al. (2007b)
Be 75	$-0.22 \pm 0.20$	40000	25–40	1 giant	EW	Carraro et al. (2007b)
Blanco 1	$+0.04 \pm 0.02$	50000	$\geq 70$	8 F-G dwarf	Syn	Ford et al. (2005)
	$+0.20 \pm 0.03$	28000	100–400	4 dwarf	EW	Edvardsson et al. (1995)
Cr 121	+0.25	20000		1 supergiant	EW	Mallik (1998)
Cr 261	$-0.22 \pm 0.11$	25000	$\geq 75$	4 giant	EW	Friel et al. (2003)
	$-0.03 \pm 0.04$	40000	70–130	6 giant	EW	Carretta et al. (2005)
	$-0.01 \pm 0.02$	47000	80–100	12 giant	EW	De Silva et al. (2007)
	$+0.13 \pm 0.05$	45000	$\geq 60$	7 giant	EW	Sestito et al. (2008)
Hyades	$+0.13 \pm 0.02$	45000	200	14 F dwarf	EW	Boesgaard & Friel (1990)
	$-0.05 \pm 0.03$	60000	$\sim 200$	29 F 19 A dwarf	Syn	Varenne & Monier (1999)
	$+0.12 \pm 0.06$	40000	100–300	3 giant	EW	Boyarchuk et al. (2000)
	$+0.13 \pm 0.08$	40000	$\sim 100$	2 F-K dwarf	EW	Sestito et al. (2003)
	$+0.13 \pm 0.06$	60000	100–200	55 F-M dwarf	EW	Paulson et al. (2003)
	$+0.13 \pm 0.05$	60000	100–200	46 F-K dwarf	EW/Syn	De Silva et al. (2006)
	$+0.14 \pm 0.04$	40000	100	1 dwarf	EW	D’Orazi & Randich (2009)
	$+0.21 \pm 0.04$	60000	175–225	3 G dwarf/4 giant	Syn	Schuler et al. (2009, 2006)
IC 2391	$-0.03 \pm 0.07$	18000–44000	30–100	4 dwarf	EW	Randich et al. (2001)
	$-0.01 \pm 0.02$	40000	70–280	7 G–K dwarf	EW	D’Orazi & Randich (2009)
IC 2581	$-0.34 \pm 0.02$	18000	$\geq 100$	1 F supergiant	EW	Luck (1994)
IC 2602	$-0.05 \pm 0.05$	18000–44000	30–100	9 dwarf	EW	Randich et al. (2001)
	$+0.00 \pm 0.01$	40000	100–250	8 G–K dwarf	EW	D’Orazi & Randich (2009)
IC 2714	$+0.12 \pm 0.09$	48000	180	1 giant	EW <sup>2</sup>	Smiljanic et al. (2009)
	$-0.01 \pm 0.01$	50000	200–300	3 giant	EW	Santos et al. (2009)
IC 4651	$+0.11 \pm 0.01$	40000	$\geq 100$	5 giant	EW	Carretta et al. (2004)

<sup>1</sup> Spectral synthesis for O.<sup>2</sup> Spectral synthesis for C, N, O.

**Table 12.** Continued.

Cluster		[Fe/H]	Resolution	S/N	N. Star	Method	References
		+0.10±0.03	45000	70–120	5 giant/18 dwarf	EW	Pasquini et al. (2004)
		+0.12±0.05	100000	~80	5 G dwarf	EW	Pace et al. (2008)
		+0.15±0.01	50000	200–300	3 giant/3 dwarf	EW	Santos et al. (2009)
		+0.11±0.01	48000	≥100	5 giant	EW/Syn	Mikolaitis et al. (2011)
IC 4665		−0.03±0.04	60000	30–150	18 F–K dwarf	Syn	Shen et al. (2005)
IC 4725	M 25	+0.18±0.08	18000	≥100	2 supergiant/1 giant	EW	Luck (1994)
IC 4756		−0.02±0.05	18000	≥100	4 supergiant	EW	Luck (1994)
		−0.15±0.04	15000	70–150	7 giant	EW <sup>3</sup>	Jacobson et al. (2007)
		+0.04±0.04	48000	≥170	5 giant	EW <sup>2</sup>	Smiljanic et al. (2009)
		+0.02±0.03	50000	200–300	3 giant/3 dwarf	EW	Santos et al. (2009)
		+0.01±0.09	100000	50–100	3 dwarf	EW	Pace et al. (2010)
		+0.08±0.11	100000	50–100	3 giant	EW	Pace et al. (2010)
M 11	NGC 6705	+0.10±0.07	38000	85–130	10 K giant	EW/Syn	Gonzalez & Wallerstein (2000)
M 34	NGC 1039	+0.07±0.04	45000	~70	9 G dwarf	EW	Schuler et al. (2003)
M 67	NGC 2682	+0.02±0.05	28000	20–50	4 F dwarf	EW	Friel & Boesgaard (1992)
		−0.03±0.03	30000	≥100	9 giant	EW <sup>4</sup>	Tautvaišienė et al. (2000)
		−0.01±0.04	28000	≥200	3 giant	EW	Yong et al. (2005)
		+0.03±0.01	45000	80–180	8 dwarf/2subgiant	EW	Randich et al. (2006)
		+0.03±0.04	100000	~80	6 G dwarf	EW	Pace et al. (2008)
		+0.00±0.02	50000	200–300	3 giant/3 dwarf	EW	Santos et al. (2009)
		+0.03±0.07	28000	150–180	3 giant	EW <sup>1</sup>	Friel et al. (2010)
		−0.01±0.05	21000	>70	19 giants	EW <sup>1</sup>	Jacobson et al. (2011b)
Mel 20	Alpha	+0.23±0.08	45000	300–450	1 supergiant/1 dwarf	EW	Gonzalez & Lambert (1996)
	persei	−0.05±0.05	45000	100	7 F dwarf	EW	Boesgaard & Friel (1990)
Mel 66	Cr 147	−0.38±0.01	30000	~100	2 giant	EW	Gratton & Contarini (1994)
		−0.33±0.03	45000	80–115	5 giant	EW	Sestito et al. (2008)
Mel 71	Cr 155	−0.30±0.01	34000	~100	2 giant	EW	Brown et al. (1996)
Mel 111	Coma	−0.05±0.05	28000	≥150	14 F dwarf	EW	Friel & Boesgaard (1992)
	Berenice	+0.06±0.10	42000	150–400	11 A 11 F dwarf	Syn	Gebran et al. (2008)
NGC 188		+0.01±0.08	35000	20–35	11 G dwarf	EW	Randich et al. (2003)
		+0.12±0.02	28000	120–140	4 giant	EW <sup>1</sup>	Friel et al. (2010)
		−0.03±0.04	21000	>70	27 giants	EW <sup>1</sup>	Jacobson et al. (2011b)
NGC 752		−0.09±0.05	40000	80–150	8 dwarf	EW	Hobbs & Thorburn (1992)
		+0.01±0.04	57000	30–80	18 G dwarf	EW	Sestito et al. (2004)
NGC 1193		−0.30±0.06	28000	100	1 giant	EW <sup>1</sup>	Friel et al. (2010)
NGC 1245		−0.04±0.05	21000	>70	13 giants	EW <sup>1</sup>	Jacobson et al. (2011b)
NGC 1817		−0.07±0.04	28000	120	2 giant	EW <sup>1</sup>	Jacobson et al. (2009)
		−0.16±0.03	21000	>70	28 giants	EW <sup>1</sup>	Jacobson et al. (2011b)
NGC 1883		−0.20±0.22	20000	~20	5 giant	EW	Villanova et al. (2007)
		−0.01±0.01	28000	~100	3 giant	EW <sup>1</sup>	Jacobson et al. (2009)
NGC 1901		−0.08±0.01	33000–64000	50–80	1 subgiant	EW <sup>1</sup>	Carraro et al. (2007a)

<sup>3</sup> Spectral synthesis for Al, Na, O.<sup>4</sup> Spectral synthesis for C, N, Eu

**Table 12.** Continued.

Cluster	[Fe/H]	Resolution	S/N	N. Star	Method	References
NGC 2112	-0.09±0.10	16000–34000	80	2 giant	EW	Brown et al. (1996)
	+0.16±0.03	33000	80–100	3 giant	EW	Carraro et al. (2008)
NGC 2141	-0.26	28000	≥130	1 giant	EW	Yong et al. (2005)
	+0.00±0.16	28000	75	1 giant	EW <sup>1</sup>	Jacobson et al. (2009)
NGC 2158	-0.03±0.14	28000	75	1 giant	EW <sup>1</sup>	Jacobson et al. (2009)
	-0.28±0.05	21000	>70	15 giants	EW <sup>1</sup>	Jacobson et al. (2011b)
NGC 2194	-0.08±0.08	21000	>70	6 giants	EW <sup>1</sup>	Jacobson et al. (2011b)
NGC 2204	-0.23±0.04	20000	≥60	13 giant	EW	Jacobson et al. (2011a)
NGC 2232	+0.22±0.09 <sup>5</sup>	16000	70–300	5 dwarf	EW	Monroe & Pilachowski (2010)
	+0.32±0.08 <sup>5</sup>	16000	70–300	5 dwarf	EW	Monroe & Pilachowski (2010)
NGC 2243	-0.48±0.01	30000	~100	2 giant	EW	Gratton & Contarini (1994)
	-0.42±0.05	20000	≥60	10 giant	EW	Jacobson et al. (2011a)
NGC 2264	-0.18±0.08	45000	45–75	4 dwarf	EW	King et al. (2000)
NGC 2324	-0.17±0.05	45000	≥80	7 giant	EW	Bragaglia et al. (2008)
NGC 2355	-0.08±0.08	21000	>70	5 giants	EW <sup>1</sup>	Jacobson et al. (2011b)
NGC 2360	+0.07±0.06	28000	50–200	4 giant	EW	Hamdani et al. (2000)
	+0.04±0.09	28000	≥70	4 giant	EW <sup>2</sup>	Smiljanic et al. (2009)
	-0.03±0.01	50000	200–300	3 giant	EW	Santos et al. (2009)
NGC 2420	-0.57±0.08	20000		4 giant	Syn	Smith & Suntzeff (1987)
	-0.20±0.06	21000	>70	9 giants	EW <sup>1</sup>	Jacobson et al. (2011b)
NGC 2423	+0.14±0.06	50000	200–300	3 giant	EW	Santos et al. (2009)
NGC 2425	-0.15±0.09	21000	>70	4 giants	EW <sup>1</sup>	Jacobson et al. (2011b)
NGC 2447	+0.03±0.03	28000	50–2000	3 giant	EW	Hamdani et al. (2000)
	-0.01±0.01	28000	≥70	3 giant	EW <sup>2</sup>	Smiljanic et al. (2009)
	-0.10±0.03	50000	100–300	3 giant/3 dwarf	EW	Santos et al. (2009)
NGC 2477	+0.07±0.03	45000	≥80	6 giant	EW	Bragaglia et al. (2008)
NGC 2506	-0.20±0.02	40000	≥35	4 giant	EW	Carretta et al. (2004)
	-0.24±0.05	48000	≥35	4 giant	EW	Mikolaitis et al. (2011)
NGC 2516	+0.01±0.07	47000	70	2 F dwarf	EW	Terndrup et al. (2002)
NGC 2539	+0.13±0.09	50000	200–300	3 giant	EW	Santos et al. (2009)
NGC 2660	+0.04±0.04	45000	≥45	5 giant	EW	Bragaglia et al. (2008)
NGC 3114	+0.05±0.13	48000		7 giant	EW	Pereira & Quireza (2010)
	+0.02±0.09	50000	200–300	3 giant	EW	Santos et al. (2009)
NGC 3532	+0.10±0.17	18000	≥100	5 giant/1 supergiant	EW	Luck (1994)
	+0.04±0.05	48000	≥170	6 giant	EW <sup>2</sup>	Smiljanic et al. (2009)
NGC 3680	-0.04±0.03	100000	~80	2 G dwarf	EW	Pace et al. (2008)
	+0.04±0.10	48000	200	1 giant	EW <sup>2</sup>	Smiljanic et al. (2009)
	-0.03±0.01	50000	200–300	3 giant/3 dwarf	EW	Santos et al. (2009)
NGC 3960	+0.02±0.04	45000	≥95	6 giant	EW	Bragaglia et al. (2008)
NGC 4349	-0.12±0.06	50000	200–300	3 giant	EW	Santos et al. (2009)
NGC 5460	+0.05±0.24	25000	≥100	21 A B F	Syn	Fossati et al. (2011)
NGC 5822	+0.07±0.02	18000	≥100	1 giant	EW	Luck (1994)

<sup>5</sup> Depending on the adopted temperature scale.



**Table 12.** Continued.

Cluster		[Fe/H]	Resolution	S/N	N. Star	Method	References
		+0.04±0.08	48000	≥130	5 giant	EW <sup>2</sup>	Smiljanic et al. (2009)
		+0.05±0.04	50000	200–300	3 giant/3 dwarf	EW	Santos et al. (2009)
		+0.05±0.09	100000	50–100	2 dwarf	EW	Pace et al. (2010)
		+0.15±0.11	100000	50–100	3 giant	EW	Pace et al. (2010)
NGC 6067		+0.02±0.12	18000	≥100	1 supergiant	EW	Luck (1994)
NGC 6087		+0.06±0.20	18000	≥100	2 supergiant/1 giant	EW	Luck (1994)
NGC 6134		+0.15±0.07	40000	≥60	6 gint	EW	Carretta et al. (2004)
		+0.12±0.09	48000	≥150	3 giant	EW <sup>2</sup>	Smiljanic et al. (2009)
		+0.15±0.05	45000	≥60	6 giant	EW <sup>1</sup>	Mikolaitis et al. (2010)
NGC 6192		+0.12±0.04	47000	≥140	4 giant	EW	Magrini et al. (2010)
NGC 6253		+0.46±0.03	48000	85–180	5 giant	Syn	Carretta et al. (2007)
		+0.36±0.07	47000	65–140	2 giant/1 subgiant/1 dwarf	EW	Sestito et al. (2007)
NGC 6281		+0.05±0.06	48000	≥230	2 giant	EW <sup>2</sup>	Smiljanic et al. (2009)
NGC 6404		+0.11±0.04	47000	≥110	4 giant	EW	Magrini et al. (2010)
NGC 6475	M 7	+0.14±0.06	48000	50–150	13 F-K dwarf	EW	Sestito et al. (2003)
		+0.03±0.02	18000	≥200	2 B 3 F-K dwarf/2 G-K giant	EW	Villanova et al. (2009)
NGC 6583		+0.37±0.03	47000	≥80	2 giant	EW	Magrini et al. (2010)
NGC 6633		+0.07±0.05	48000	≥160	2 giant	EW <sup>2</sup>	Smiljanic et al. (2009)
		+0.06±0.01	50000	200–300	3 giant	EW	Santos et al. (2009)
NGC 6791		+0.37±0.03	20000	30	1 hot HB	EW/Syn	Peterson & Green (1998)
		+0.35±0.02	25000	≥40	6 giant	Syn	Origlia et al. (2006)
		+0.38±0.02	20000	30–60	10 giant	Syn	Carraro et al. (2006)
		+0.47±0.07	29000	40–85	4 giant	Syn	Carretta et al. (2007)
		+0.30±0.08	45000	~40	2 dwarf	EW	Boesgaard et al. (2009)
NGC 6819		+0.09±0.03	40000	130	3 giant	EW	Bragaglia et al. (2001)
NGC 6882/5		−0.03±0.01	18000	≥100	1 supergiant/1 dwarf	EW	Luck (1994)
NGC 6939		+0.00±0.10	15000	70–150	9 giant	EW <sup>3</sup>	Jacobson et al. (2007)
NGC 7142		+0.08±0.06	15000	70–150	6 giant	EW <sup>3</sup>	Jacobson et al. (2007)
		+0.16±0.01	30000	100–130	4 giant	EW <sup>1</sup>	Jacobson et al. (2008)
NGC 7160		+0.16±0.03	16000	70–300	16 F-G dwarf	EW	Monroe & Pilachowski (2010)
NGC 7789		−0.04±0.05	30000	≥50	9 giant	EW/Syn	Tautvaišienė et al. (2005)
		+0.02±0.04	21000	>70	28 giants	EW <sup>1</sup>	Jacobson et al. (2011b)
Pleiades	M 45	−0.03±0.02	45000	150	12 F dwarf	EW	Boesgaard & Friel (1990)
		−0.03±0.10	18000–44000	30–100	2 dwarf	EW	Randich et al. (2001)
		+0.06±0.02	42000–75000	100–300	16 A giant/5 F dwarf	Syn	Gebran & Monier (2008)
		+0.07±0.03	45000	70	2 dwarf	EW	King et al. (2000)
		+0.07±0.05	40000		20 F-G-K dwarf	Syn	Soderblom et al. (2009)
Praesepe	M 44	+0.04±0.04	28000	60–190	6 F dwarf	EW	Friel & Boesgaard (1992)
	Mel 88	+0.27±0.04	100000	~130	7 G dwarf	EW	Pace et al. (2008)
Rup 4		−0.09±0.04	40000	25–40	3 giant	EW	Carraro et al. (2007b)
Rup 7		−0.26±0.05	40000	25–40	5 giant	EW	Carraro et al. (2007b)
Saurer 1		−0.38±0.01	34000	~80	2 G giant	EW	Carraro et al. (2004)
To 2		−0.50±0.10	34000	50–60	3 giant	EW	Brown et al. (1996)
		−0.28±0.01	21000–40000	15–70	18 giant	EW	Frinchaboy et al. (2008)

**Table 12.** Continued.

Cluster	[Fe/H]	Resolution	S/N	N. Star	Method	References
	$-0.31 \pm 0.02$	17000	60–80	13 giant	EW	Villanova et al. (2010)
Tr 20	$-0.11 \pm 0.13$	50000	65	1 giant	EW	Platais et al. (2008)